Chapter 3
Sintering by High-Voltage Electric Pulses

3.1 Principle and Physical Mechanisms of High-Voltage Consolidation

Consolidation of powders by high-voltage electric pulses generally attracts attention as a method of very fast consolidation, in which most of the heat is released at the inter-particle contacts. High-voltage electric pulse sintering is a processing of choice when refractory metals are to be consolidated [1–3]. The principle of this technique is the passage of a high-voltage current pulse through the powder sample under applied external pressure. In the most widely used variation of high-voltage consolidation, the current is produced by discharging a capacitor bank. The described sintering methods utilize electric discharges of several kV, electric current densities exceeding 10 kA·cm^{-2}, and pressures of up to 10 GPa. In most cases, the powder to be consolidated is subjected to a single electric pulse with duration shorter than 0.1 s. Consequently, electric pulse methods allow consolidating near-net-shape powder compacts much faster than in the conventional methods of densification, such as pressureless sintering, hot pressing, or hot isostatic pressing. Fast sintering in high-voltage techniques can be thought of as a possibility to conduct sintering with minimal microstructure changes, if those are undesirable in the consolidated material. Belyavin et al. [1] approached electric current-assisted sintering pursuing the sintering enhancement possibilities of refractory metals. The activation of sintering by current was suggested as more efficient than the activation by the introduction of low-melting-temperature additives.

Pulse consolidation processes exist in several variations: high-voltage electric discharge consolidation (HVEDC) [4–10], high-energy high-rate consolidation (HEHR) [11–16], pulse plasma sintering (PPS) [17, 18], and capacitor discharge sintering (CDS) [19–23]. A setup for HVEDC uses pulsed current generated by discharging a capacitor bank to rapidly heat the powder sample, to which external pressure is simultaneously applied. The main parameters of the HVEDC process are the external pressure and the electric current generated by the discharge. In HEHR

E. A. Olevsky, D. V. Dudina, *Field-Assisted Sintering*,
https://doi.org/10.1007/978-3-319-76032-2_3

consolidation, a homopolar generator is used, which transforms the rotation energy into the electrical energy as a result of Faraday's effect. Although the HEHR method uses a voltage below 100 V, it is often discussed together with high-voltage consolidation due to its highly dynamic nature: consolidation by means of a single pulse of a very high electric current (100–500 kA). In PPS, a current source generates periodical pulses of current. Sintering is conducted in vacuum, which differs this method from other methods based on the application of pulsed current. The CDS method uses two circuits coupled by mutual inductance instead of a single RLC circuit. This configuration allows applying low voltages to the powder compact, thus reducing the possibilities of discharges, breakdown, and local plasma formation during the process. The CDS normally produces nearly fully dense compacts, the porosity being present only in the surface layer and uniformly distributed. The CDS method is based on the storage of high-voltage electrical energy in a capacitor bank inserted in a freely oscillating system composed of a primary circuit and a mutually coupled secondary circuit. The secondary circuit works in conjunction with a mechanical press, which is controlled by a programmed logical controller. Once the desired pressure from the press is reached, the switch closes the circuit, and the electromagnetic energy is transferred to the secondary circuit by means of a transformer that enables conversion from high voltage and low current in the primary circuit to low voltage and high current in the secondary circuit. A comprehensive review by Yurlova et al. [1] summarizes the current knowledge of the process mechanisms and tracks the historical development of the high-voltage methods. The advantages of HVEDC can be exploited only through the optimization of the consolidation parameters since excessive energy dissipation during this type of processing can lead to the instability of the compaction process, the formation of an undesirable material structure, and even to the destruction of the sintered specimens and of the equipment used. The time dependence of the associated thermal processes at the inter-particle contacts plays a key role in electric pulse powder consolidation.

A schematic of a HVEDC setup, an equivalent electric diagram, and HVEDC tooling are shown in Fig. 3.1. The behavior of the electric circuit consisting of a capacitor, a consolidation setup, and a powder column is described by the following equation [10, 24]:

$$\frac{d^2U}{d\tau^2} + \frac{R(\tau)}{L}\frac{dU}{d\tau} + \frac{U}{LC} = 0, \tag{3.1}$$

where U is the voltage, τ is the time, L is the inductance, and C is the capacitance. The principal difficulty in describing the process of HVEDC mathematically is the changing resistance of the powder compact during the process. If $R^2(\tau) > 4LC$, i.e., the resistance of the powder compact exceeds the reactive component of the circuit, the discharge has an aperiodic character. If $R^2(\tau) < 4LC$, the discharge is a damped oscillation process. Electric discharge consolidation facilities usually use a Rogowski coil to measure the current and oscillographs to record the current waveform. The typical current waveform during HVEDC is a damped sinusoid (Fig. 3.2)

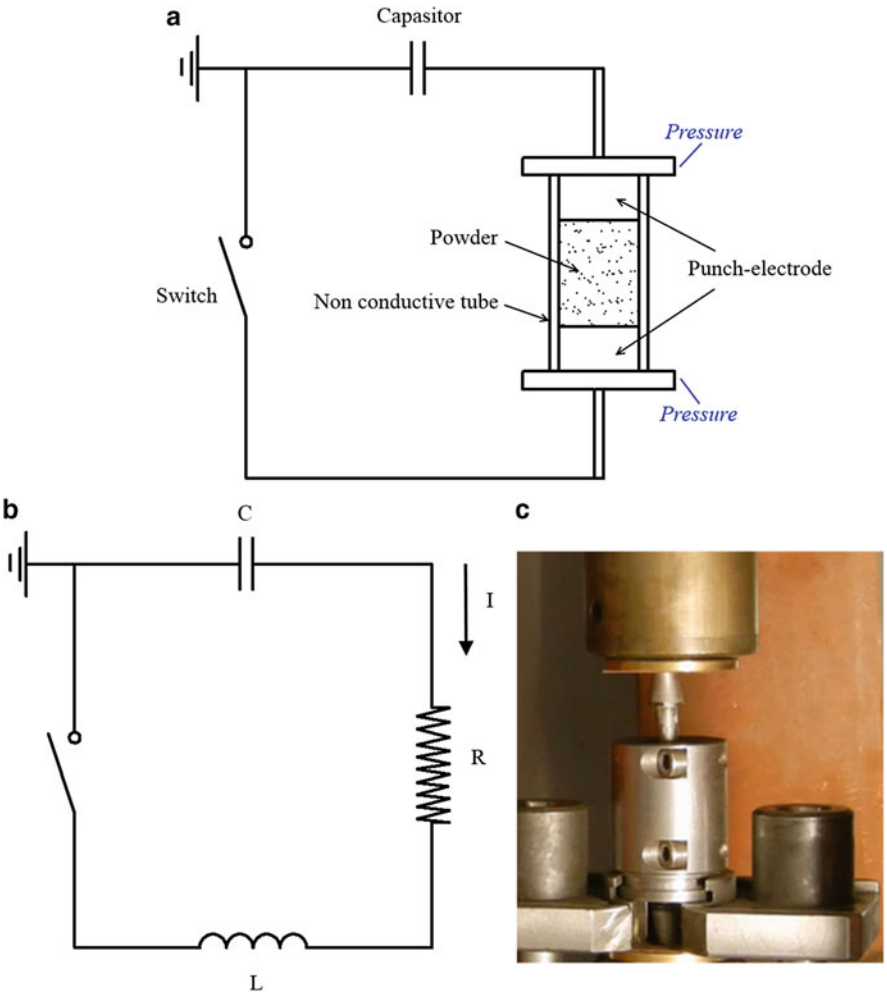

Fig. 3.1 Schematic of a HVEDC setup (**a**), equivalent electric diagram (**b**), and HVEDC tooling (**c**)

[25]. A change from a damped oscillation discharge to an aperiodic discharge (Fig. 3.3) can be caused by an increase in the compact resistance due to temperature rise due to Joule heating [24].

Al-Hassani et al. [26] suggested using the electric circuit theory to describe the electric pulse sintering. The mathematical model is based on the assumption that the inductance and capacitance remain constant, while the resistance varies with temperature. The variation of resistance with time during electric discharge sintering is expressed by a two-term exponential form:

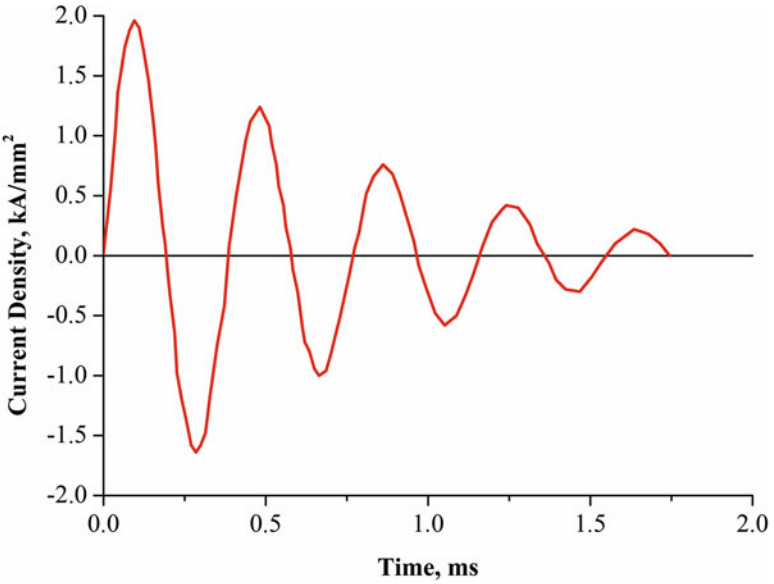

Fig. 3.2 Typical pulse current waveform during HVEDC (Rogowski coil) [25]

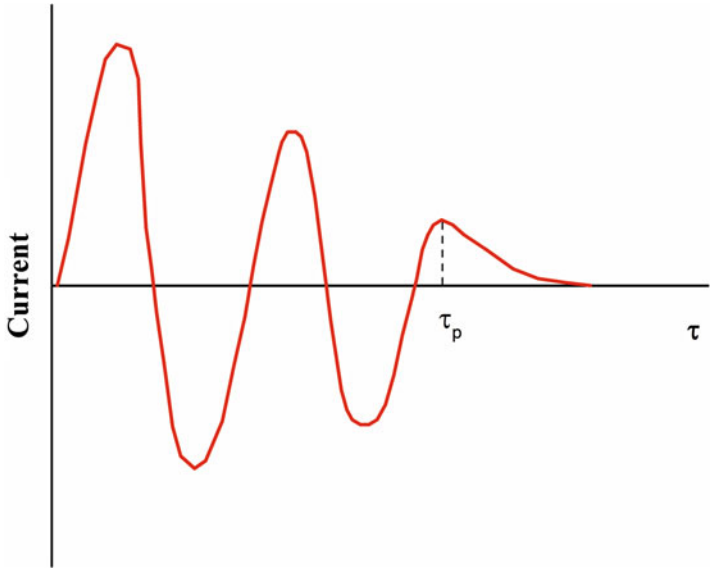

Fig. 3.3 A change from a damped oscillation discharge to an aperiodic discharge [24]

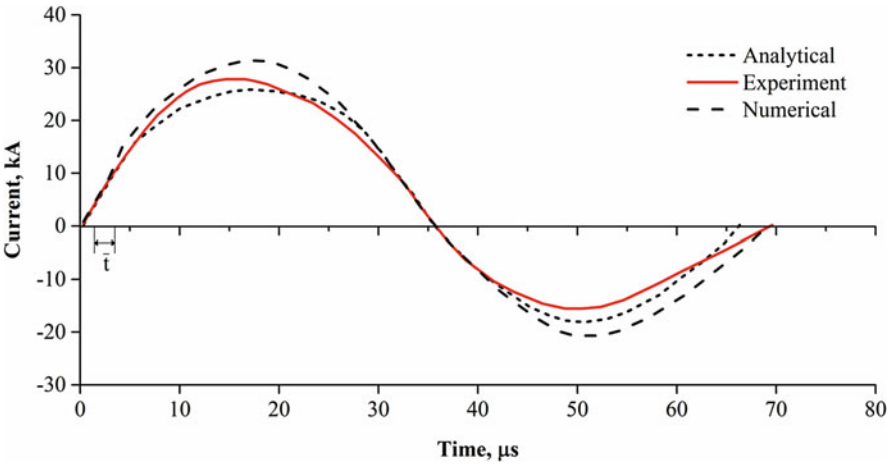

Fig. 3.4 Current waveforms of a commercial steel powder sample. (Reprinted from Al-Hassani et al. [26], Copyright (1986) with permission from Elsevier)

$$R(t) = R_1(t) + R_2(t) \text{ where } R_1 = A_1 e^{-\alpha_1 t} \text{ and } R_2 = A_2 e^{-\alpha_2 t} \text{ here } A_1 \gg A_2, \alpha_1 \gg \alpha_{21} \tag{3.2}$$

Assumption (3.2) implies that when t is small, the first term $R_1(t)$ dominates, and when t is large, the second term does. A mathematical analysis of the equations was carried out to determine the time dependence of the electric current. As is seen in Fig. 3.4, the calculations are in good agreement with the experimental results [26].

The experimental results on the instantaneous resistance of three steel powders oxidized for different periods of time are presented in Fig. 3.5 [27]. The resistance of the powder column shows an initial sharp reduction, which is consistent with the breakdown of the insulating oxide layers on the particle surfaces. In the subsequent stage of consolidation (after the breakdown of the oxide layers), the powder resistance slightly increased, apparently due to an increase in temperature. It can be seen that the instantaneous resistance of the powder column depends on the thickness of the oxide film. As can be concluded from Figs. 3.5 and 3.6, the resistance of the compacts is dramatically reduced by the time the current reaches its maximum.

In order to exclude heating of the sample throughout its volume, the electric pulse duration should be shorter than the time needed to heat the materials through heat conduction. Short pulses lead to the skin effect and the formation of thin skin layers. In order to ensure the uniform heating of the sample through its cross section, the thickness of the skin layer should be greater than the characteristic size of the sample. The pulse duration should be shorter than the time needed to fully heat the particles; otherwise complete melting of the sample might take place. The pulse duration should satisfy the relationship:

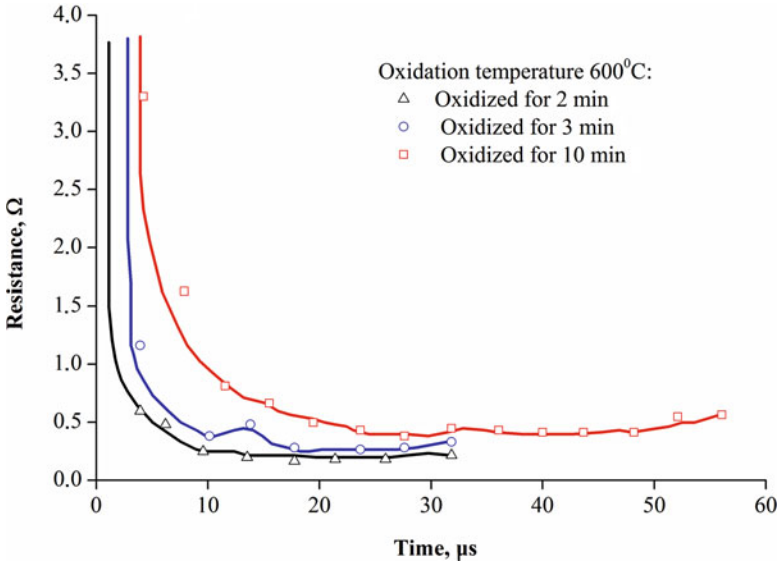

Fig. 3.5 Evolution of resistance of oxidized steel powders during electric pulse consolidation. (Reprinted from Alitavoli and Darvizeh [27], Copyright (2008) with permission form Elsevier)

$$\tau_M < \tau_P \ll \tau_T, \tag{3.3}$$

where τ_P is the pulse duration, τ_M is the time, during which the magnetic field penetrates the sample determined by the skin effect, and τ_T is the time needed to heat the powder particles [29]. These two characteristic times depend on the material properties, the sample dimensions, and the particle size of the powder. The sample electrical resistance during electric pulse sintering usually changes according to the following scenario: during the first 10–20 μs, the electrical resistance rapidly drops, then it decreases more slowly, and after 100–200 μs from the process start, the resistance stops decreasing and may as well increase due to heating of the sample. The faster the discharge, the shorter the time, during which the electrical resistance levels off. Zavodov et al. shortened the discharge duration by using exploding wires [29]. It was shown that sintering can occur within a time as short as ~2 μs. The sintered material did not, however, possess the required strength.

The characteristic cooling time in electric pulse sintering is several seconds. The duration of the densification process is several milliseconds [30]. Based on this, densification can be assumed to occur at a constant temperature. The analysis of the electric pulse sintering parameters reveals the hierarchy of the characteristic times in the electric pulse sintering process. The energy input into the powder material is characterized by the pulse duration $\tau_0 < 10^{-3}$ s. The time, during which the compact is formed from the powder, depends on the mechanical loading system and lies in the $2 \cdot 10^{-3} < \tau_1 < 2 \cdot 10^{-2}$ s range. The cooling time of the sintered sample τ_2 is a

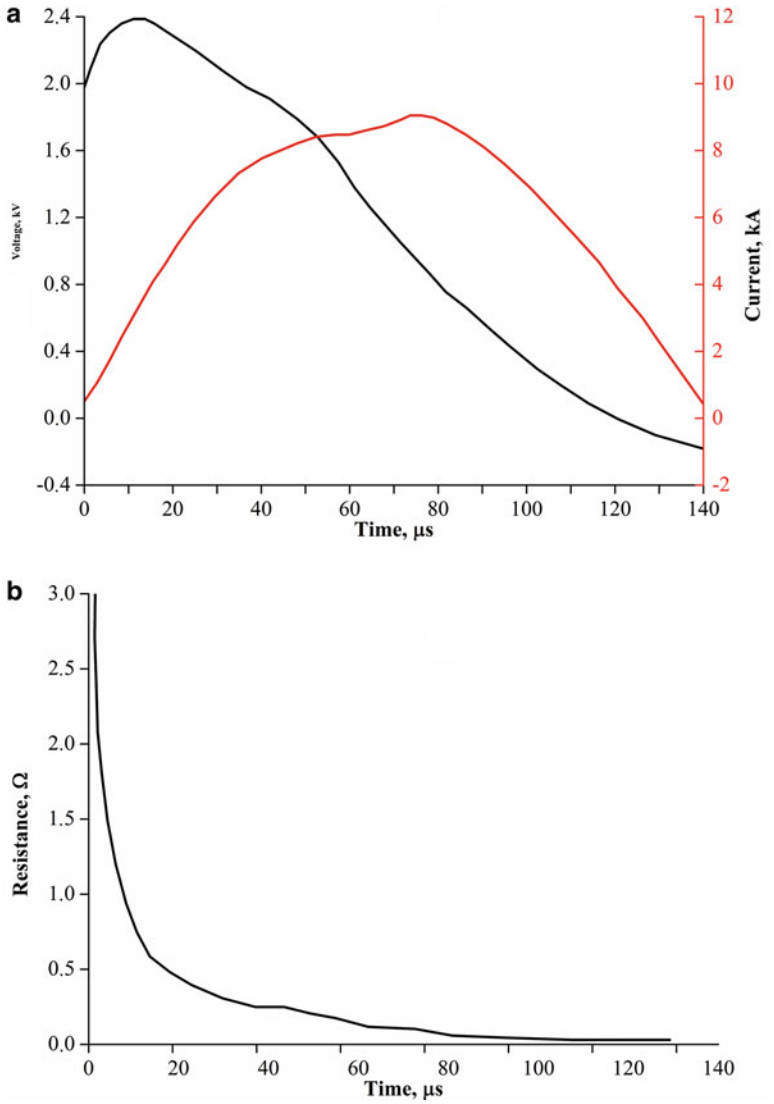

Fig. 3.6 Voltage and current (**a**) and resistance (**b**) of a compact consolidated from an oxidized nickel powder by an electric discharge. (Reprinted from Kim et al. [28], Copyright (1988) with permission from Elsevier)

function of thermal conductivity of the material and the characteristic sample size; $\tau_2 \approx 2.5$ s. The following relationship is observed: $\tau_0 < \tau_1 \leq \tau_2$ [5, 30].

The pinch effect causing constriction of the powder sample in the radial direction is observed only at certain current values passing through the sample during the discharge. When the electric current is uniformly distributed over the cross section of

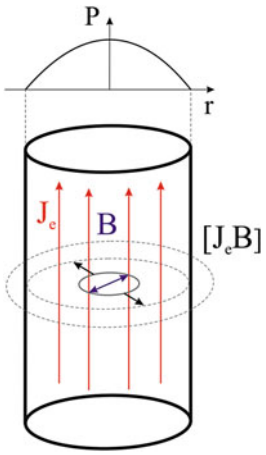

Fig. 3.7 The pinch effect in a powder sample during electric pulse sintering and magnetic pressure p profiles

a cylindrical powder sample of radius r_0, the magnetic pressure can be calculated using equation [31]:

$$p_m(r) = -\frac{\mu_0\left(r_0^2 - r^2\right)I^2}{4\pi^2 r_0^4} \tag{3.4}$$

where μ_0 is the vacuum permeability, r is the radial distance, and I is the current. The action of the pinch effect is schematically shown in Fig. 3.7. The distribution of the magnetic pressure over the sample cross section is of a parabolic character with a maximum in the center of the sample.

The action of magnetic pressure can produce a nonuniform pore distribution in the porous powder material. However, if

$$p_l \geq p_m, \tag{3.5}$$

where p_l is the pressure on the lateral surface of the compact caused by the compressive force applied to the electrode, this will not take place [10]. If $p_l = p_m$, the friction force will be zero between the powder compacts and the die wall.

The distribution of the magnetic pressure is more uniform when a strong skin effect is observed. The pinch effect makes it easier to take the sintered sample out the die; the repeated use of the die is possible reducing the processing costs. The greater is the length of the sample, the lower is the current, and the lower is the pressure caused by the pinch effect. This consideration explains a reduction in the sintered density of samples with increasing their length.

Kim et al. [28] reported microscopic evidence of heavy deformation of nickel as a result of electric discharge consolidation carried out without external pressure and suggested that this deformation was caused by electromagnetic forces generated during the discharge. The indications of heavy deformation were observed microscopically as cells with small-angle boundaries.

3.2 Stages of High-Voltage Consolidation

As was already mentioned, an important feature of high-voltage electric pulse sintering is the concentration of the released energy in the contact zone between the particles. Therefore, the initial state of the powder particles (the thickness and structure of oxide films, the presence of second-phase inclusions, etc.), the shape and size of the particles, as well as the applied pressure greatly influence the physical processes during the consolidation, which are spatially inhomogeneous and time-dependent.

Al-Hassani et al. distinguish five sintering stages [32]:

- Destruction of the surface contaminating layers between the adjacent particles in the axial direction upon the critical applied stress depending on the nature of the powder material and geometry of the sample; this is accompanied by an instantaneous drop in the sample resistance and an increase in the current passing through the paths of least resistance.
- Inter-particle sintering leading to the formation of inter-particle necks parallel to the direction of electric current; the inter-particle necks grow, and this is accompanied by a further reduction in electrical resistance; however, an increase in the resistivity with temperature can be significant, and it is possible that the total resistance of the powder sample will increase.
- At the third stage, the conductive inter-particle necks are self-constricted as a result of the pinch effect; the surface layers of the particles are destroyed in the radial and azimuthal directions, which lead to sintering of the particles to each other in these directions.
- The electric current passes through the continuous metal using the previously formed electrical paths.
- Disintegration and stability loss or electric explosion.

In powder compacts, the density fluctuations, which can often be present due to powder agglomeration, can cause fluctuations in electrical conductivity within the compact. The paths of least resistance can be overheated. If overheating results in the formation of a molten metallic channel, a short circuit forms leaving the rest of the sample poorly sintered. Working with a mixture of steel and polyethylene powders, Alp et al. [33] determined a critical voltage, above which the compact disintegrates in a similar way a metallic wire explodes under a high current.

Fundamental parameters of electric pulse sintering are the specific energy input (SEI) and applied pressure. According to Ervin [34], SEI is the result of the real part of the current and real part of the voltage acting on the sample:

$$\mathrm{SEI} = \lim_{t\to+\infty} \frac{E_\mathrm{j}(t)}{w} \approx \frac{1}{w}\int_0^{t^*} i(\tilde{t})\cdot v(\tilde{t})\,d\tilde{t}, \tag{3.6}$$

где $E_\mathrm{j}(t)$ is the energy used to heat the powder (Joule effect); w is the mass of the powder placed in the die; t^* is an approximate discharge duration; $i(t)$ and $v(t)$ are

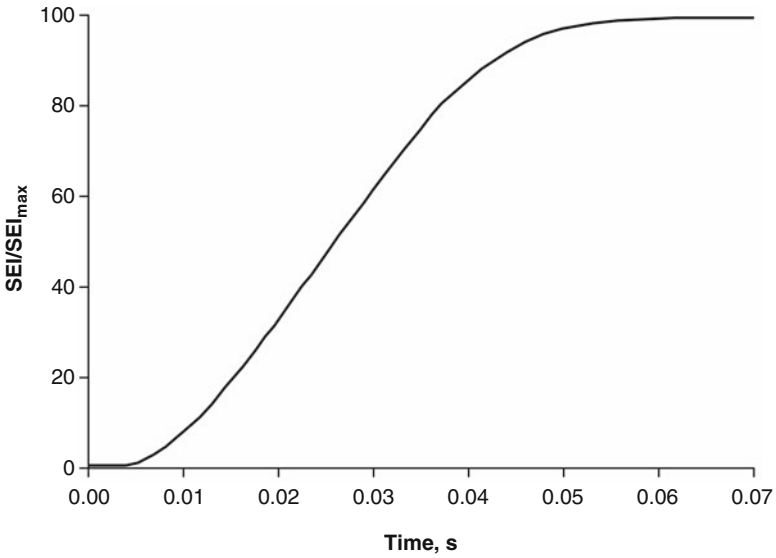

Fig. 3.8 Variation in time of the energy dissipated during an electric pulse in CDS due to Joule effect. (Reprinted from Fais [21], Copyright (2010) with permission from Elsevier)

electric current and voltage during the discharge. For instance, the typical pulse duration in capacitor discharge sintering is 30 ms, and 90% of the energy is released in less than 20 ms (Fig. 3.8). Higher values of SEI can lead to higher compact densities [21]. The thermal cycle lasts about 1 s [20].

In order to characterize an electric pulse sintering process, Anisimov and Mali [35] used the integral of current:

$$J = \int_0^t j^2 dt \tag{3.7}$$

where j is the current density in the sample. Sintering occurs when the integral of current exceeds a critical value, which is lower than required to fully melt the material.

3.3 Processes at Inter-particle Contacts During High-Voltage Consolidation

When no electric current is involved in the sintering process, the densification rate will increase with increasing applied pressure; however, in electric pulse sintering, as the level of pressure influences the resistance of the powder compact, an opposite influence may be expected. As the pressure increases, the contact resistance between the particles decreases reducing Joule heating. Al-Hassani has found that the

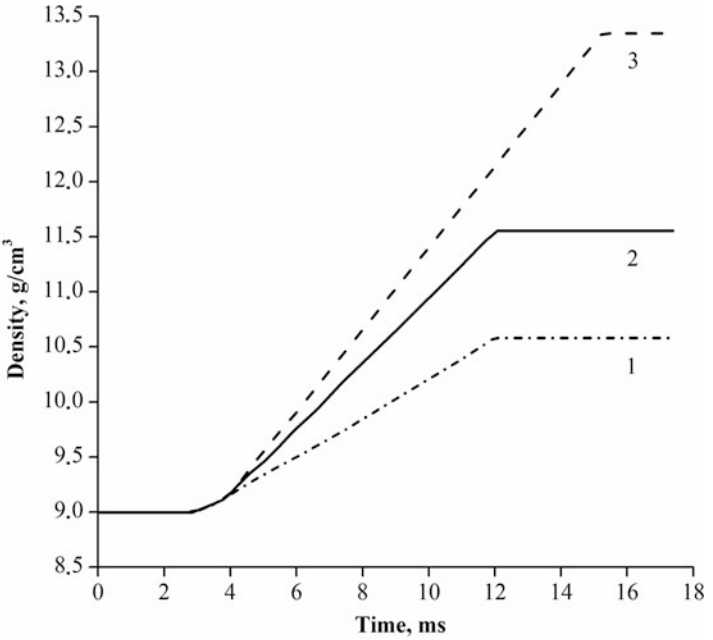

Fig. 3.9 Variation of the sample density with time during electric pulse sintering of WC–Co powders: 1 – 75 kA cm^{-2}, 2 – 85 kA cm^{-2}, and 3 – 97 kA cm^{-2} at a constant applied pressure of 150 MPa. (Reprinted from Grigoryev [6], distributed under Creative Commons Attribution 3.0 Unported License (CC BY 3.0), https://creativecommons.org/licenses/by/3.0/)

resistance of the powder volume is inversely proportional to $P^{2/3}$; here P is the axial pressure applied to the powder sample [26]. The yield strength of the material decreases with temperature; therefore, the lower is the temperature of the material, the higher is its yield strength, and, consequently, the lower is its densification rate. At a constant initial resistance of the powder compact ensured by the same applied pressure, the temperature of the inter-particle contacts increases with increasing current density and the powder consolidation rate increases, as shown in Fig. 3.9 for WC–Co compacts [6]. At a constant pulsed current, the densification rate is determined by the temperature dependence of the yield strength of the material. Grigoryev [4, 6] proposed using a dimensionless parameter $\beta = \sigma(T)/P$, where $\sigma(T)$ is the yield strength of the material, to analyze the change in the densification rate with applied pressure. Indeed, the pressure determines the initial resistance of the powder column and the amount of heat released in the powder material as well as its temperature. With an increase in the pressure, the resistance of the powder column decreases, and the heating of the material is reduced. Normally, a higher external pressure leads to a higher consolidation rate. However, a direct pressure-associated increase in the consolidation rate is leveled by the temperature dependence of the yield strength of the powder material in the case of consolidation assisted by a current pulse, as the sample's temperature does not remain constant (Fig. 3.10).

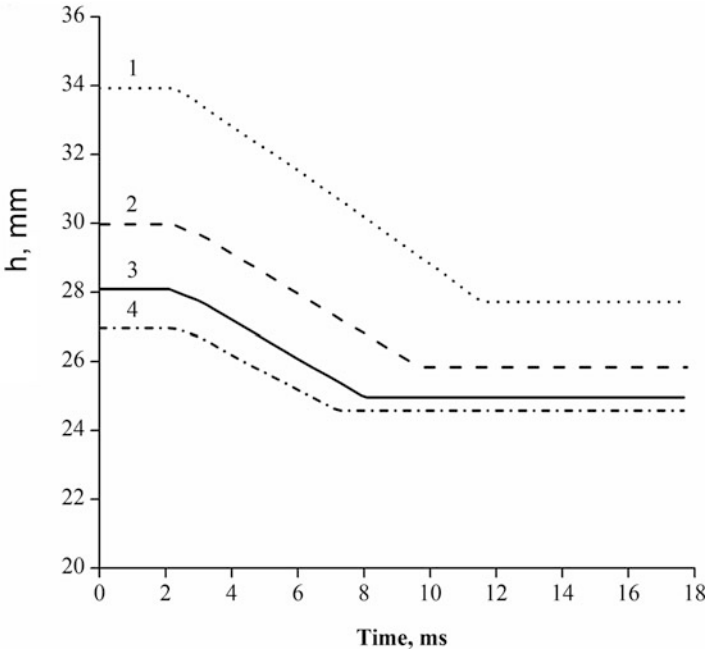

Fig. 3.10 Variation of the sample height with time during electric pulse sintering of an iron powder for a fixed current density (156 kA cm^{-2}) and different pressures: (1) 106 MPa, (2) 176 MPA, (3) 247 MPa, (4) 282 MPa. (Reprinted from Grigor'ev [4], Copyright (2008) with permission of Springer)

The pressure distribution along the vertical axis of the sample is shown in Fig. 3.11 [1]. Such a character of the pressure distribution is caused by the friction between the powder and the walls of the die. The difference in the applied pressure causes differences in the resistance, and, consequently, heat evolved in the compact. For parts of significant lengths, a multistep process has been suggested, in which new "portions" of a powder are "added" to the rod by means of sintering.

Belyavin et al. [1] consider the behavior of molten columns (bridges) that form between the particles during electric pulse sintering. Under the combined action of the applied mechanical pressure, electromagnetic forces, and surface tension, the bridges can change their shape, lose their stability, and move away from the contact area. The dependences of the size of the inter-particle contacts and porosity and strength of titanium compacts are shown in Fig. 3.12. When a certain pressure is reached, the molten bridges lose their stability, and some molten metal flows away from the compact. The capillary and electromagnetic forces are responsible for the stability of molten bridges, while the internal hydrostatic pressure of the liquid column can induce squeezing of the melt from the inter-particle contact. When this happens, the contacts are reduced in size and the mechanical strength of the sintered compact decreases. Figure 3.12b shows that there is an optimal pressure that should

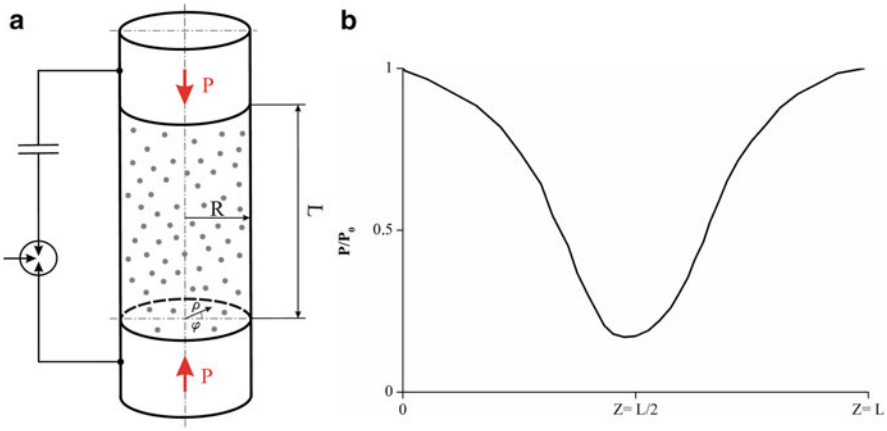

Fig. 3.11 Pressure distribution along the sample length [1]

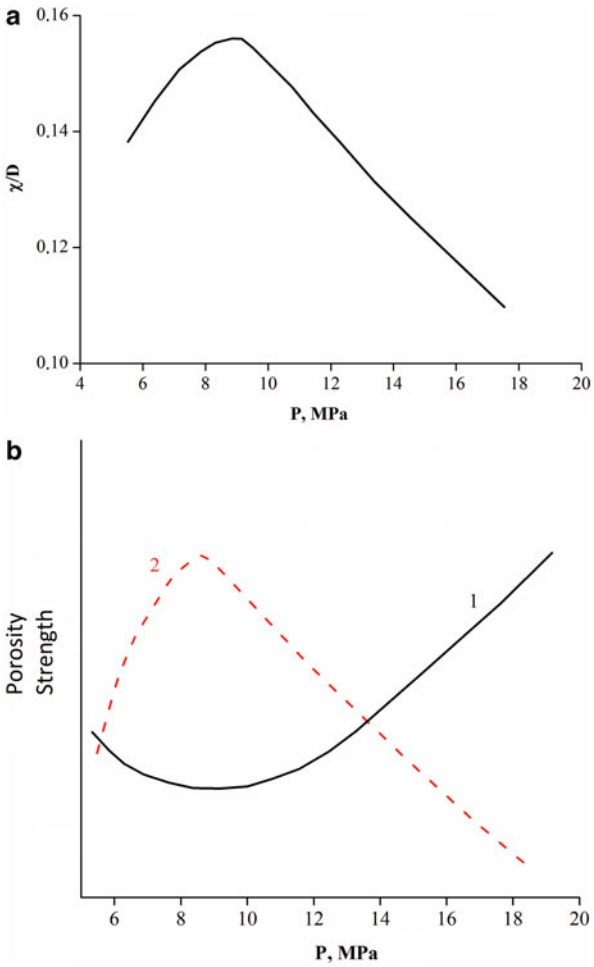

Fig. 3.12 Relative size of the inter-particle contacts (**a**) and porosity (1) and strength (2) of the compacts (**b**) vs. applied mechanical pressure for titanium compacts. (Drawn using data of Ref. [1])

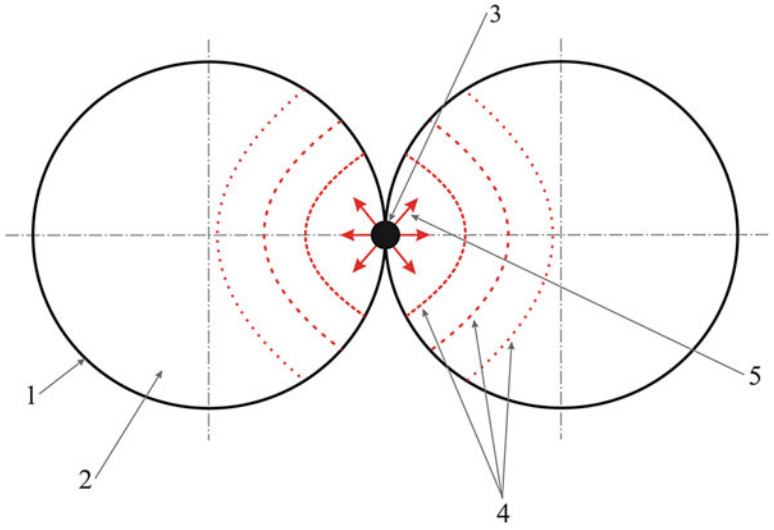

Fig. 3.13 The heat exchange scheme between the heated layers of the contacting powder particles (1, oxide film; 2, powder particle; 3, contact zone; 4, isotherms; 5, heat dissipation direction). (Reprinted from Belyavin et al. [10], Copyright (2004) with permission of Springer)

be applied to maximize the compact strength and minimize the porosity. If no pressure is applied, the electric pulse-sintered compacts are only 40–70% dense.

An important sintering factor is the temperature of the sample. The neck size between the particles was shown to increase with the heat generated in the sample during the pulse [36]. Belyavin et al. have found a relationship between the discharge voltage and the temperature of the powder particles [10]. The following assumptions have been made:

- The heat in the contact zones of all powder particles evolves uniformly; the heat exchange processes occur independently of each other.
- Due to short discharge durations, there is no heat exchange with the surroundings.
- The particles are heated from the heat sources, which are the contact zones.
- The contact zone is a semisphere.
- The dissipation of heat inside the particle occurs according to the scheme of Fig. 3.13; the heat is distributed between the particles equally.
- Heat exchange between the inner layers of the particles is governed by Fourier's law.

Figure 3.13 shows the scheme of the heat exchange between the heated layers of the powder particles. The temperature in the contact zone is determined by [10]:

$$T_q = \frac{3q - 2.25b\gamma\pi d^3}{4(c_1 + c_2)\gamma\pi d^3}, \tag{3.8}$$

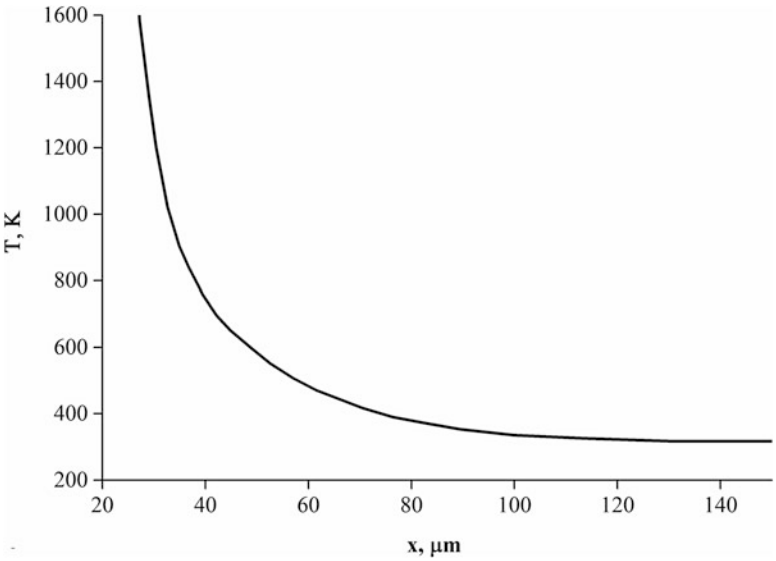

Fig. 3.14 The temperature inside a powder particle vs. the distance from its surface. (Reprinted from Belyavin et al. [10], Copyright (2004) with permission of Springer)

where T_q is the temperature in the contact zone, b is the specific melting heat, c_1 and c_2 are the heat capacities of the solid and liquid state of the material, d is the diameter of the contact zone, γ is the density of the particle, and q is the specific discharge energy. The characteristic temperature variation inside a powder particle with distance from the particle surface is shown in Fig. 3.14. An advantage of electric pulse sintering is the evolution of heat in the contact zone between the particles, which leaves the central regions of the particles relatively cold.

The temperature at the inter-particle contacts depends on the angle between the contact zone and the direction of electric current. In the contact zones normal to the direction of electric current, the temperature is the highest, while in the contact zones parallel to the direction of electric current, the temperature may not increase at all.

The temperature of the contact zone between the particles can be calculated by incorporating current distribution into the random packing of particles [37]. The following assumptions are made: the particles are incompressible, the Joule heat is not dissipated by radiation or conduction, and the particle surface becomes clean of the surface oxide before the peak current is reached (the surface cleaning time is much shorter than the discharge time). The temperature of each contact zone can be calculated using the following equation [38]:

$$\Delta T_i = \int_0^{t_p} [j \cos(\theta_i)]^2 \rho / (dc) dt \tag{3.9}$$

where ΔT_i is the temperature in i contact zone, t_p is the pulse duration, j is the microscopic current density, θ_i is the solid angle between the normal to the contact

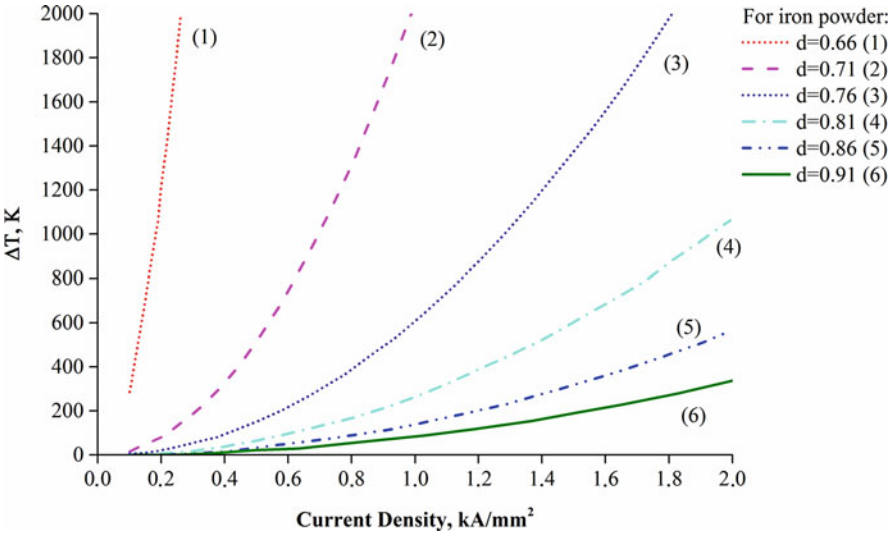

Fig. 3.15 Temperatures at the inter-particle contacts calculated by Wu and Guo [25] for iron compacts of different relative density. (Reprinted from Wu and Guo [25], Copyright (2007) with permission of Springer)

surface and the direction of the current, ρ is the resistivity, d is the density of the bulk material, and c is the heat capacity.

At the contact area perpendicular to the current direction, the temperature is the highest. Wu and Guo [25] calculated the average temperatures of the inter-particle contacts using the following equation:

$$\Delta T = \overline{\Delta T_i} = \sum\nolimits_1^{Z/2} (\cos\ \theta_i)^2 \int_0^{t_p} j^2 \rho/(dc) dt, \tag{3.10}$$

where Z is the average coordination number in the pressing limit, which, as was shown by Artz [37], depends on the relative density D:

$$\begin{aligned} Z(D) &= Z_0 + 9.5(D - D_0) \text{ for } D < 0.85, \\ Z(D) &= Z_0 + 2 + 9.5(D - 0.85) + 881(D - 0.85)^3 \text{ for } D > 0.85, \end{aligned} \tag{3.11}$$

where $Z_0 = 7.3$ is the initial coordination number. The calculation results for iron compacts of different relative density (66–91%) are presented in Fig. 3.15. The temperature is sensitive to the relative density and increases with increasing current density dramatically at low relative densities. Calculations of the average temperatures at the contact regions allow determining whether a substantial role in densification will be played by liquid-phase sintering mechanisms. The role of liquid phases in the densification of tungsten heavy alloys by electric discharge is demonstrated in Fig. 3.16, from which it can be concluded that as the content of tungsten in

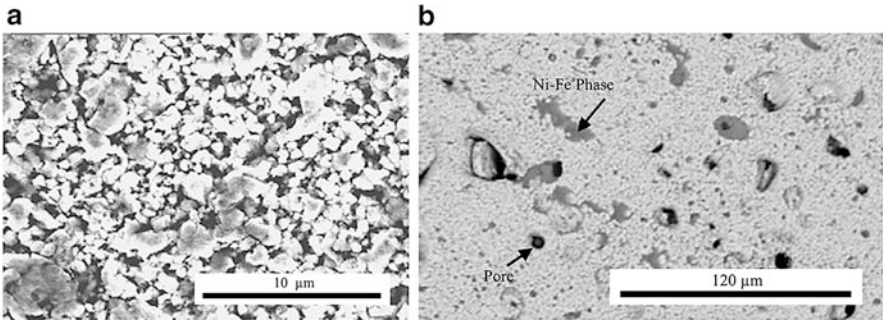

Fig. 3.16 Microstructure of W–Ni–Fe alloys consolidated under the same current density (2.5 kA mm^{-2}): (**a**) 98W–Ni–Fe, (**b**) 90W–Ni–Fe. (Reprinted from Wu and Guo [25], Copyright (2007) with permission of Springer)

the alloys decreases, the densification becomes more efficient and the evidence of the liquid-phase sintering is seen as areas in the microstructure corresponding to the Ni–Fe phase.

The nature of thermal processes in the inter-particle contacts has a significant influence on the temperature distribution throughout the volume of the consolidated material. Experimental results show that generation of an insufficient local Joule heat in the inter-particle contacts leads to weak intergranular bonding, a low final density, and a low mechanical strength of the consolidated specimen. On the other hand, during HVEDC, there is an upper critical level for the local Joule heating of the inter-particle contacts, beyond which the powder material disintegrates like an exploding wire [33]. Therefore, the optimum electric pulse current amplitude and pulse time length are necessary to generate a sufficient amount of heat for the stable formation of strong inter-particle bonds.

Grigoryev and Olevsky [5] developed a mathematical model of the physical processes occurring under HVEDC, taking into account the processes in the particle contact zones, which is described below. The system of equations describing the processes under HVEDC was based on the mass, momentum, and energy conservation laws and on the electrodynamic equations for the consolidated powder materials. Simulation of the HVEDC confirmed two different time scales for the thermal processes occurring during the processing: the first stage – the stage of the energy input into the powder, and the second (final) stage (the stage of cooling) of the consolidated material. The numerical results indicated the possibility of the localization of heat in the inter-particle contacts for certain parameter values of the high-voltage pulse electric current. The simulation of the thermal processes in the inter-particle contacts has identified an upper critical level for the high-voltage pulse current amplitude, beyond which the inter-particle contacts in the powder material disintegrate via an electrothermal explosion:

$$j_o = \sqrt{\frac{2\xi\sigma}{\rho h}} T_\mathrm{b}, \tag{3.12}$$

where $\xi \leq 1$, σ is the Stefan–Boltzmann constant, T_b is the boiling point of the material, ρ is the electrical resistivity of the contact spot, and h is the thickness of the contact area. Equation (3.12) was obtained from the analysis of the heat balance at the initial period of time when the electric current density rapidly increases during the pulse (at its leading edge). The heat balance assumes the equivalence of the Joule heat generation rate and the heat dissipation by heat transfer through radiation.

Belyavin et al. [1] calculated the depth of the molten region at the inter-particle contacts and cooling rates of the molten material after the completion of the pulse. The depth increases with increasing energy of the discharge and decreases with increasing pulse duration (Fig. 3.17). Figure 3.18 shows the cooling rate variation with time for different distances from the particle surface for a titanium powder. It can be seen that immediately after the completion of the process (the pulse duration was 50 μs), the cooling rates as high as 10^8 K s^{-1} are achieved and remain at a level of 10^6 K s^{-1} for about 10 μs. Such cooling rates favor the formation of a fine-grained structure or amorphous zones at the inter-particle contacts.

High energy density in the contact zones can bring about changes of the state of the material (solid into liquid and partially into a dense low-temperature plasma). Vityaz' et al. [39] studied the distribution of the alloying elements across the contact formed between the spherical particles of a Ti alloy, in which α and β phases were present, stabilized by Al and Mo alloying elements, respectively. It was found that during conventional vacuum sintering, a uniform distribution of the alloying elements was established, while in electric pulse sintered compacts, concentration "jumps" were observed when moving from one particle to another indicating a far-from-equilibrium state of the material in the neck region formed in the conditions of highly localized and rapid heat release.

The microstructural evidence of higher temperatures of the particle outer layers relative to the interior and the occurrence of melting/rapid solidification processes was obtained by Cho et al. [40], who used a metallic glass powder, which crystallized with increasing temperature. A spherical metallic glass powder of the $Cu_{54}Zr_{22}Ti_{22}Ni_6$ composition with particles ranging from 5 to 45 μm was sintered by a single capacitor discharge, and the microstructure of the porous compact was studied. While morphological changes of the particle surfaces are usually accepted as the evidence of melting and solidification in the systems of crystalline metals, a grainy structure was to indicate the thermally induced crystallization processes in the sintered metallic glass powder. The crystallized outer layer of the particles 30–45 μm in diameter observed along with an unchanged amorphous core indicated higher temperatures of the particle surfaces. Smaller particles crystallized completely. When the energy of the pulse was sufficient to fully crystallize the material, there was still a difference in the microstructure of the outer regions of the particles and that of the core, the grains being smaller in the former due to faster cooling.

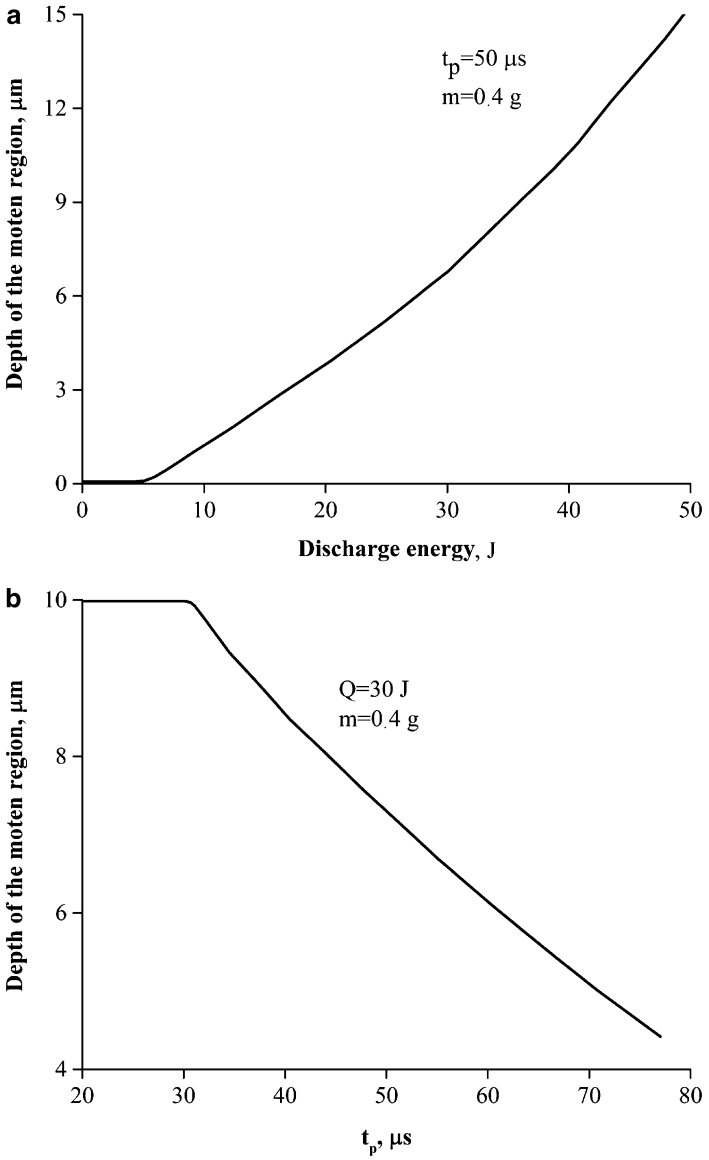

Fig. 3.17 Depth of the molten region at the inter-particle contacts vs. discharge energy (**a**) and duration of the pulse (**b**) for a titanium powder. (Drawn using data of Ref. [1])

The role of diffusion during electric pulse sintering is not fully understood. Fais argues that atomic diffusion plays the major role, but the interaction of thermal, electromagnetic, and mechanical fields makes it challenging to analyze the processes [21]. However, Wu and Guo point out that diffusion and viscous flow are negligible during electric pulse sintering owing to extremely short sintering durations [25].

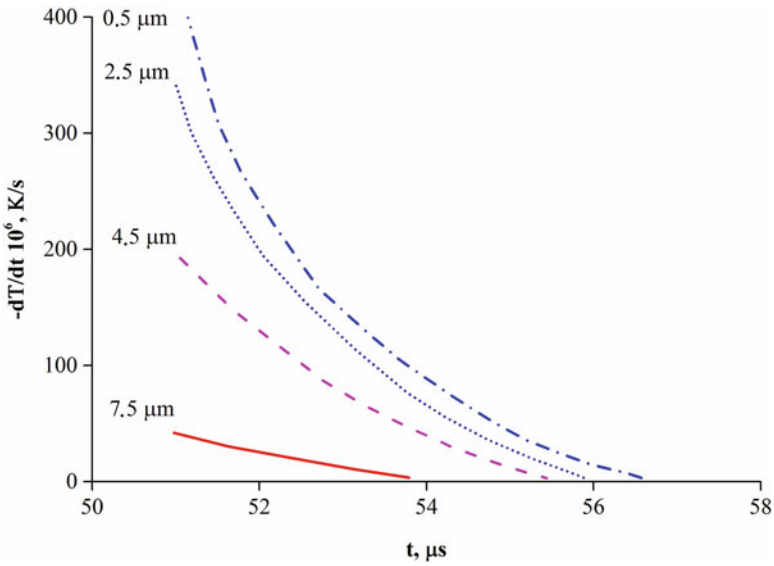

Fig. 3.18 Calculated cooling rates vs. time for different distances from the particle surface for a titanium powder. (Drawn using data of Ref. [1])

The possibility of improving the quality of the sintered compacts by applying several high-voltage pulses has been a matter of discussion. Belyavin found that a porous compact forms during the first discharge [10]. Zavodov et al. studied the effect of the voltage application mode and of the number of pulses on the quality of the sintered samples [29]. The voltage was increased with each subsequent pulse. It was found that when the voltage was gradually increased, the final resistance of the materials was 2–3 times lower than in the case of a single pulse. The neck diameter was 30–50% of the particle diameter. The strength of the material sintered using this step-by-step voltage increase approach was higher than the strength of the material sintered by a single pulse.

The efficiency of electric pulse sintering is the ratio of the thermal energy released in the powder compact during the discharge to the electrical energy stored by the capacitor bank. In order to increase the efficiency of electric pulse sintering facilities that can be described by a simple oscillatory RLC circuit, Belyavin et al. [10] derived a relationship, which, if observed, guarantees that during the first period of oscillations, the major fraction of the stored energy of the capacitor (95%) is released as heat:

$$\sqrt{\frac{L}{C}} \leq R < \sqrt{\frac{2L}{C}} \tag{3.13}$$

where R is the resistance, L is the circuit inductor, and C is the capacitance of the capacitor bank.

Applying modeling methods, the circuit parameters can be found such that the efficiency calculated using Eq. (3.13) would be the highest:

$$\eta = (1-\delta)\frac{R_1}{\sqrt{R_1^2 + \left(\frac{1}{\omega C} - \omega L\right)^2}}, \tag{3.14}$$

where R_1 is the resistance of the powder column, ω is the frequency of the damped oscillations, η is the efficiency, and $\delta = 0.05$ is the damping factor. In order to achieve a reasonable efficiency of electric pulse sintering, a RLC circuit should possess a certain resistance.

Assuming that the particles have spherical shape, the diameter of the contact area between the particles is much smaller than the particle diameter and the particles deform elastically under a compressive force applied to the punches, Belyavin et al. analytically derived the following equation to calculate the initial resistance of the powder compact pre-pressed prior to sintering [10]:

$$R = \rho \frac{4D_0}{\pi(1-2\varepsilon)^2 n_V^{1/3}} \left(\frac{E}{3FD_0(1-\nu^2)(1-\sigma)}\right)^{2/3} \frac{h}{S}, \tag{3.15}$$

where ρ is the resistivity of the material of the powder particles, D_0 is the particle diameter, ε is ratio of the thickness of the oxide film to the linear deformation, n_V is the volume concentration of inter-particle contacts in the compact, F is the compressive force of the electrode, E is the Poisson ratio, σ is the friction coefficient, E is the Young's modulus, h is the height, and S is the cross-sectional area of the powder compact.

The discharge efficiency is proportional to the ratio of the powder surface resistance to the sum of the circuit resistance and that of the powder surface. Rock et al. [41] suggested mixing Nb–Al mechanically milled powders produced by low- and high-energy mechanical milling to achieve a certain resistance of the compact to be sintered by electric discharge sintering. The XRD patterns of the compacts of different initial resistances are shown in Fig. 3.19. Slightly narrower peaks in the XRD patterns of higher initial resistance compacts indicate a small degree of grain growth caused by heating during the discharge. However, it is normally accepted that the duration of an electric discharge is sufficient for densification of the powders but too short for any noticeable grain growth during electric pulse sintering [1, 23].

The size of the powder particles is also important for electric pulse sintering. Zavodov et al. [29] have observed fine particles to be thrown out of the die due to intensive gas evolution during a high-voltage electric pulse [29]. The electrical conductivity of a fine powder is lower than that of a coarse powder. However, the coarse powders are consolidated into compacts of higher densities, which is related to the discharge energy dissipating between a smaller number of contacts so that each contact receives more energy at a constant discharge energy [42].

Alitavoli and Darvizeh [27] discussed the existence of the optimal thickness of the oxide film on metallic powders required to produce sufficient heat for the neck

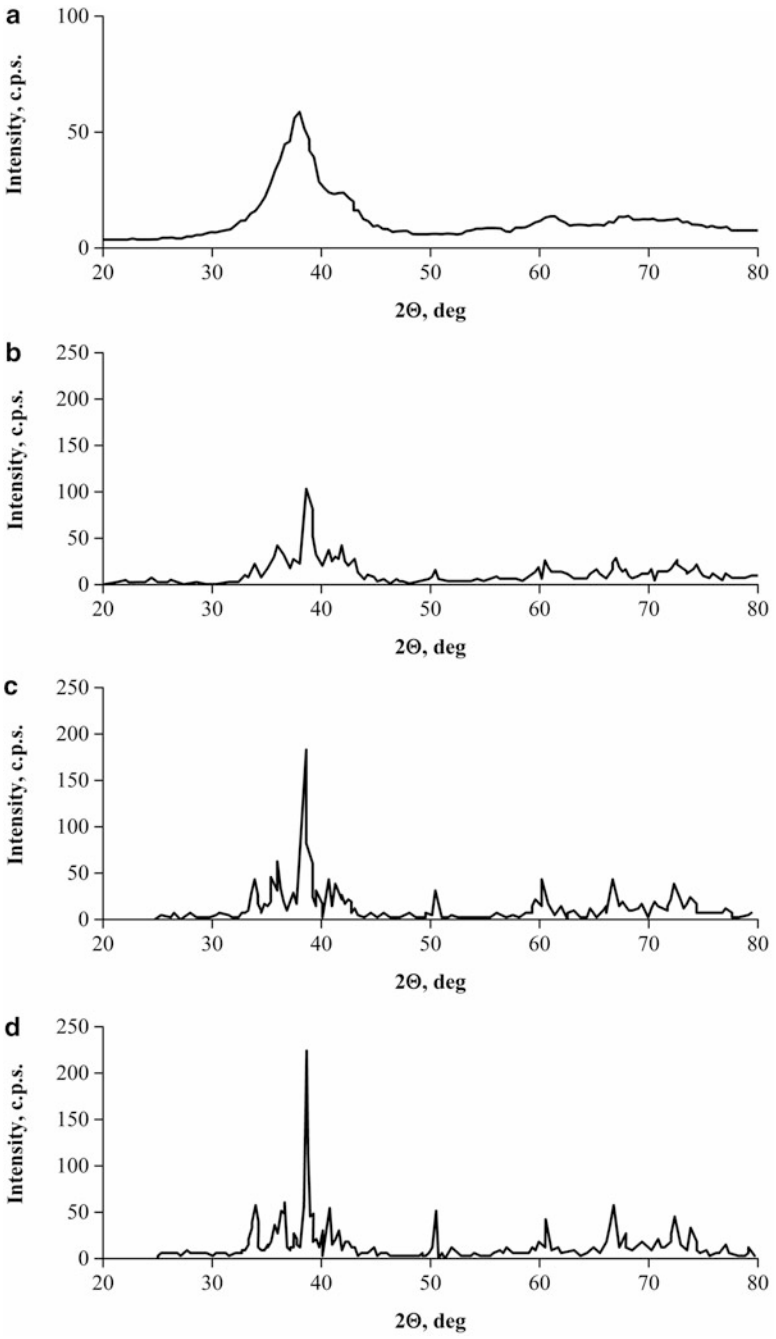

Fig. 3.19 XRD patterns of the Nb–Al powder and Nb-Al compacts of different initial resistances consolidated using the same input energy of 0.5 kJ g^{-1}: (**a**) mechanically milled mixture of Nb and Al, (**b**) 80 mΩ, (**c**) 100 mΩ, (**d**) 130 mΩ. (Reprinted from Rock et al. [41], Copyright (1998) with permission of Springer)

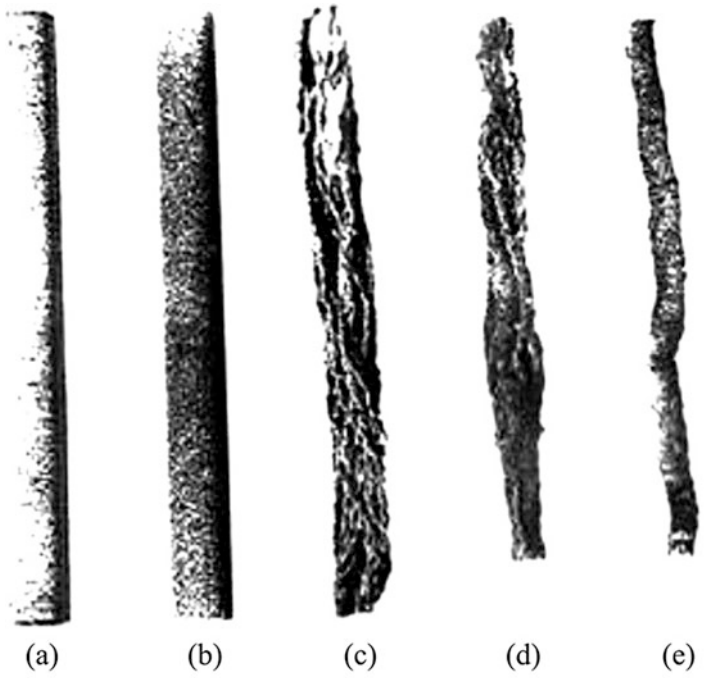

Fig. 3.20 The effect of preliminary oxidation of the steel powder on the structure of the compact: non-oxidized powder (**a**), oxidized at 500 °C for 15 min (**b**), 30 min (**c**), 40 min (**d**), and 60 min (**e**). (Reprinted from Alitavoli and Darvizeh [27], Copyright (2008) with permission from Elsevier)

formation during electric pulse consolidation. The compacts produced by hydrogen-annealed steel powders showed lower bending strength compared with those produced from the as-received powders. When the oxide film was completely removed, insufficient amounts of heat were generated, which led to weak inter-particle bonding and low mechanical strength. On the other hand, when the thickness of the oxide layer increases and the critical value is reached, the current distribution in the powder volume becomes very nonuniform such that uniform densification cannot be achieved even at the expense of an increased voltage or capacitance of the capacitor bank. Figure 3.20 shows the effect of preliminary oxidation of steel powders on the structure of the compact [27].

Figure 3.21 shows the contact areas of spherical Mo powder particles formed by the action of a constant compressive pressure of 80 MPa and of heat sources of various intensities [5]. The action of the heat sources of lower power locally enhances the plasticity of the material and causes the subsequent intense deformation of the contact region (Fig. 3.21a). A more powerful heat source leads to the local melting of inter-particle contacts and to a high rate of crystallization refining the grain structure of the material of the contact region (Fig. 3.21b).

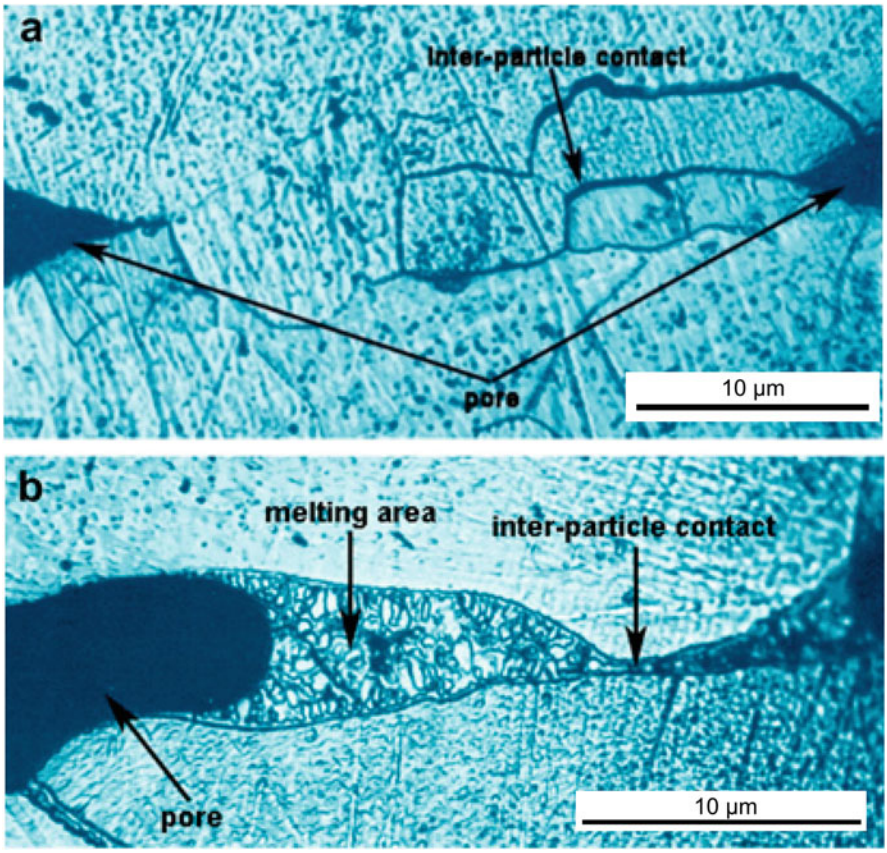

Fig. 3.21 Plastic deformation (**a**) and melting (**b**) of the contact region between Mo particles. (Reprinted from Grigoryev and Olevsky [5], Copyright (2012) with permission from Elsevier)

Electric pulse sintering is promising for making not only dense compacts but also porous materials and parts, such as filters, getters, acoustic and radio absorbers, and implants. Thus, when energy exceeding 1 kJ is evolved in the backfill of a titanium powder, a dense core forms in the center, while the adjacent material remains porous [43]. The core diameter depends on the energy at a constant charge of the capacitor bank. This effect is observed due to the action of magnetic field during the discharge (the pinch effect), which contracts the sample in the radial direction and reduces the sample diameter [44]. The porosity of the sample depends on the sintering parameters and can be varied according to the aim of the experiment. Belyavin suggests that manufacturing of porous refractory metals by electric pulse sintering will allow reducing energy consumption, make the technology more simple, and ensure the desired structural properties (porosity, pore size, specific surface area), hydrodynamic properties (permeability coefficient, local permeability), and physical and mechanical properties (strength, electrical conductivity) [45].

Investigations comparing the sintering results achieved by different methods using one and the same powder material are quite rare. Due to well-known difficulties of reliably measuring the sintering parameters, it is nearly impossible to make a direct comparison of the sintering conditions and conclude on the dominant role of a certain experimental parameter. However, by sintering the same powder by different techniques, it is still possible to conduct comparative studies. Scardi et al. [22] and Fais et al. [23] have made an attempt to find certain characteristics of the microstructure development and the crystalline structure evolution typical to CDS and spark plasma sintering (SPS) producing dense samples from the same powder. They found that due to a short sintering time in CDS, the dislocations present in the mechanically milled powder remain quite uniformly distributed in the crystalline lattice of the sintered material, while in the SPS-produced samples, the dislocations tend to interact, form pile-ups, and reach lower-energy configurations. The coherently scattering domains are smaller in the CDS samples than in the SPS ones of the same composition and having close values of density [23]. In a Fe-based alloy (Fe–1.5 wt.% Mo) sintered by CDS, austenite was found as a minor phase, while it was not present in the SPS samples of the same composition, the latter consisting of the ferritic phase. The authors conclude that in terms of preserving the nanocrystalline state of metals, the CDS method appears to be more successful.

3.4 High-Voltage Electric Discharge Consolidation (HVEDC) Apparatus

A single electric pulse passing through the powder sample of high resistance carries energy that is enough to sinter many materials. Therefore, electric pulse sintering can have its applications and advantages over the other electric current-assisted sintering techniques, such as spark plasma sintering (SPS) [1]. However, the best use of the advantages of the high-voltage electric pulse sintering can be achieved only through the optimization of the consolidation parameters. A variety of apparatus have been developed to conduct electric pulse sintering. Many facilities are unique such that their only users are their developers. Commercial manufacturing of the facilities is also rapidly developing making them available for research purposes.

The high-voltage electric discharge consolidation (HVEDC) [4, 9] setup developed in Moscow Engineering Physics Institute (MEPhI) is shown in Fig. 3.22. The setup includes an energy storage unit, a switchboard, a pressing unit, and measuring systems of electric pulse parameters, sample temperature, and densification kinetics. The energy storage unit contains a capacitor bank with a stored energy of 75 kJ, which during the discharge ensures a powerful energy release in the powder, and a charging unit. The capacitor bank contains 30 capacitors each with a capacitance of 200 μF; voltages as high as 6 kV can be achieved. The switch board in the setup is a vacuum discharger (trigatron switch), which is used to complete the circuit. The trigatron switch allows current pulses of up to 10^6 A. The setup uses pulsed current

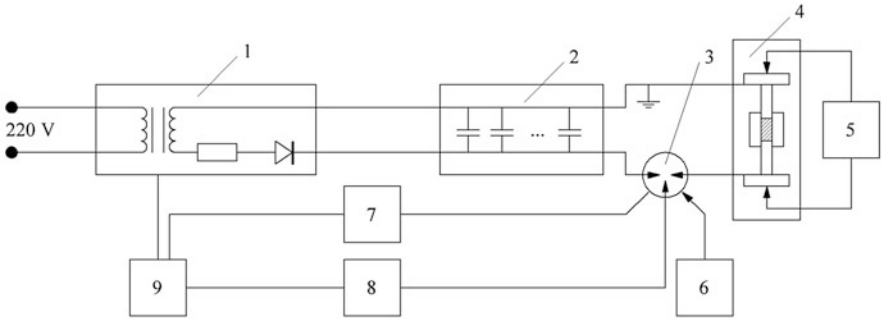

Fig. 3.22 HVEDC setup developed in Moscow Engineering Physics Institute (MEPhI): (1) charging unit, (2) capacitor bank, (3) trigatron, (4) press form, (5) pressure system, (6) current pulse recorder, (7) forevacuum pump, (8) ignition unit, (9) control unit [4, 9]

generated with the capacitor bank to rapidly heat the powder sample, to which external pressure is simultaneously applied during the sintering process. The main parameters of HVEDC are the external pressure and the electric current generated by the discharge. The powder is poured into a nonconducting ceramic die and pressed by two molybdenum punches also serving as electrodes. The powder volume ("column") is a cylinder ~10 mm in diameter and 10–15 mm high. A modification of this configuration exists featuring a ceramic tube, in which the powder is placed. In order to prevent it from damage, the tube is then placed into a metallic die. The punches, which are at the same time the electrodes, transfer pressure to the powder with the help of a pneumatic system and serve as current leads bringing electric pulses to the powder sample. The applied pressure reaching 400 MPa is created by an air-operated press or an air cylinder developing a force of 50 kN. The high-voltage capacitor bank is discharged through the powder.

The measuring system records the current amplitude and the pulse waveform in the discharge circuit of the setup. The discharge current is measured using a Rogowski coil, which is placed around the powder column. The pulse duration for this setup does not exceed 600 μs. This value determines the time, during which the energy is transferred to the powder. The temperature on the powder surface is measured by thermocouples. The weighed powder is placed inside the tooling consisting of a ceramic die and molybdenum punches, which is then set in the pressing equipment. The pressure generated by the air cylinder is controlled by a pressure gauge. Using this pressure, the powder is pre-compacted. Then the capacitor bank is charged up to a selected voltage. The trigatron receives a triggering pulse, the electric circuit closes, and the capacitor bank discharges through the pre-pressed powder material. The pressure is then released allowing the consolidated part to be taken out of the pressing equipment. The HVEDC process does not use any protective atmosphere or vacuum. Rogowski coils are usually used to measure the current, and oscillographs are used to record the current waveform. Typical temperature variations of the side surface of the powder column and the outer surface of the die during HVEDC at a constant pressure are shown in Fig. 3.23.

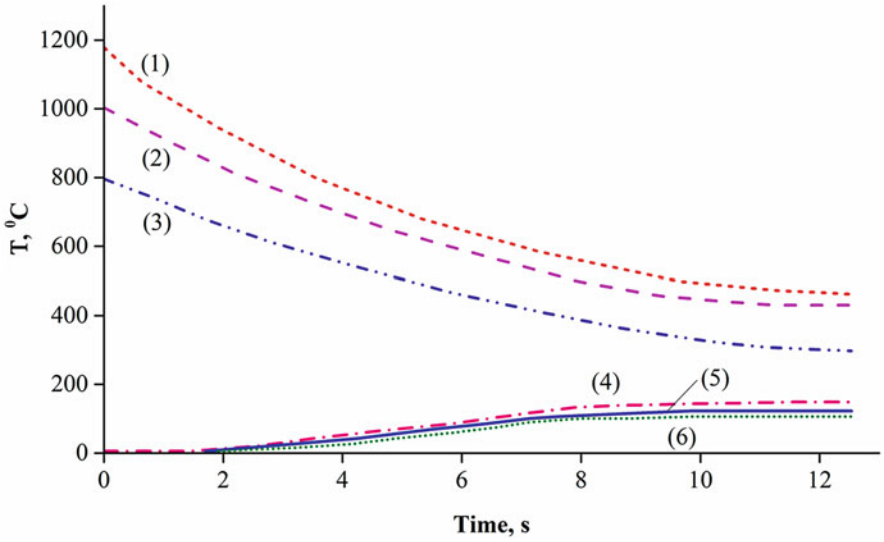

Fig. 3.23 Typical temperature variations of the side surface of the powder column (1–3) and the outer surface of the die – insulating tube (4–6) during HVEDC at a constant pressure (thermocouple method). Curves (1) and (4) were obtained at an amplitude of current density of 234 kA cm^{-2}, (2) and (5) at 195 kA cm^{-2}, (3) and (6) at 156 kA cm^{-2}. (Drawn using data of Ref. [9])

A different variation of the electric pulse sintering setup has been developed by Anisimov and Mali [35]. The powder material is pressed between two punches in a die made of fabric-based laminate. A force of 20 kN is applied by a screw press. Sintering is performed as a result of the discharge of a capacitor bank with a capacitance of 3.4 mF and a voltage of 5 kV. The discharge consists of two half-periods of current; the current amplitude in the second half-period is three times lower than that in the first one. The sample diameter can be varied from 5 to 10 mm and its thickness from 2 to 3 mm.

Electric discharge consolidation is also possible to implement in a setup, in which the direction of current is normal to the pressure application axis. Such a design was suggested by Anisimov and Mali (Fig. 3.24) [35]. The current density in the sample was sufficient to sinter compacts with dimensions of $2 \times 20 \times 30$ mm^3. In order to increase the pressure during sintering, an electromagnetic inductor was used utilizing the same current that passes through the sample or working from an additional capacitor bank. The magnetic pressure reaches 500 MPa at an inductor current of 300 kA. The inductor experiences significant damage and survives only a single experiment. The values of the current integral required for sintering measured for this geometry are close to those obtained for a conventional loading scheme.

Sintering of a powder by electric current passing directly through the sample is only possible when the powder material is electrically conductive. It is known that upon heating semiconductor materials can become conductive. An important characteristic affecting the sintering process is the sample resistance [46].

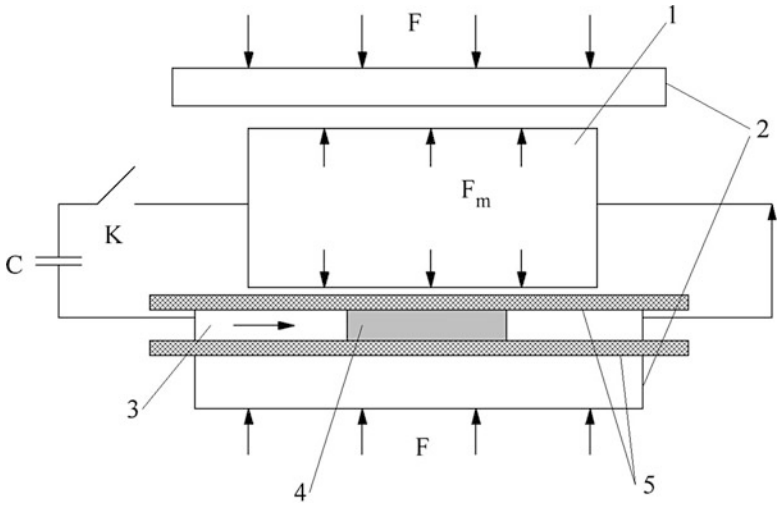

Fig. 3.24 Electric discharge sintering setup: 1, electromagnetic inductor; 2, plunger; 3, electrode; 4, powder sample; 5, insulator; C, energy storage capacitor; K, switch. (Reprinted from Anisimov and Mali [35], Copyright (2010) with permission of Springer)

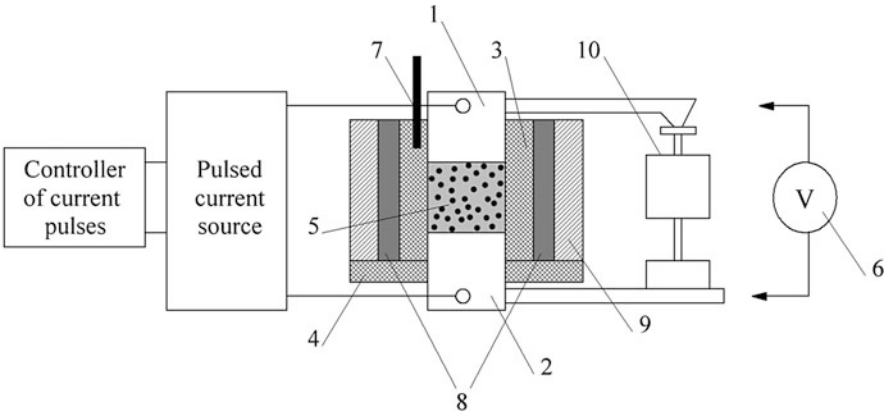

Fig. 3.25 Schematic of the electric pulse sintering setup designed to produce SiC-based ceramics: 1, 2, electrodes; 3, die; 4, insulator; 5, powder; 6, voltmeter; 7, thermocouple; 8, heating element; 9, steel binding; 10, pressure measuring unit. (Based on Ref. [47])

Bilalov et al. [47] tried to sinter silicon carbide and aluminum nitride powders by electric current using a setup shown in Fig. 3.25. The consolidation was performed in insulating dies made of sapphire; the punches served as current leads. The powders of SiC and AlN were loosely poured into the die. A high-power pulse generator was the current source. Unlike other electric pulse sintering facilities, this one includes a heating element to heat the powder prior to sintering.

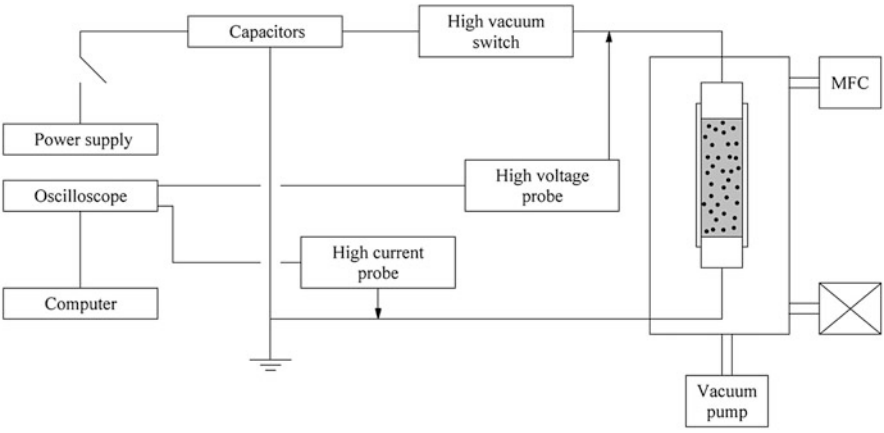

Fig. 3.26 Environmental electro discharge sintering (EEDS) setup. (Reprinted from An et al. [49], Copyright (2005) with permission from Elsevier)

Jung et al. [48] have patented a method of making porous titanium implants by electric discharge consolidation. Pyrex dies of different shapes including complex ones with cavities and arcs were used. The die is connected to copper or brass electrodes. The power supply of 100 or 200 V is used in this setup. By means of a transformer, the voltage is increased up to 1–5 kV (the preferable value is 2.5 kV). The current of a high voltage passes through the first switch and charges the capacitor. After that the capacitor is instantaneously discharged through the powder column. The consolidated samples are dense in the center and porous in the outer regions.

High chemical reactivity of titanium causes the formation of an oxide film on the surface of the Ti powder particles. To tackle this issue, a modified electric discharge consolidation setup was developed [43, 49, 50, 51]. The alterations included the addition of a vacuum system, automatic insertion of electrodes, a heat sink system, and a high-vacuum switch (Fig. 3.26). This modified consolidation method was named "environmental electro discharge sintering" (EEDS).

The vacuum system allows creating residual pressures of $2 \cdot 10^{-3}$ torr. After pumping, the discharge chamber is filled with argon up to a pressure of 1000 torr to create an inert atmosphere. The EEDS method opens up new opportunities to modify the surface of the consolidated materials. An et al. [49] used nitrogen as the gaseous environment and observed the formation of titanium nitride on the surface of the compact. The setup uses a quartz die of 4 mm diameter, tungsten cathodes, and copper heat sink elements. The upper electrode has an automatic drive. The powder is poured into the die and subjected to vibrational packing. No external pressure is applied during the sintering process.

Alp et al. have suggested a hybrid consolidation method – electro impact compaction (EIC), in which the material is subjected to a DC current prior to electric discharge consolidation [52]. This combination of the two processes resulted in

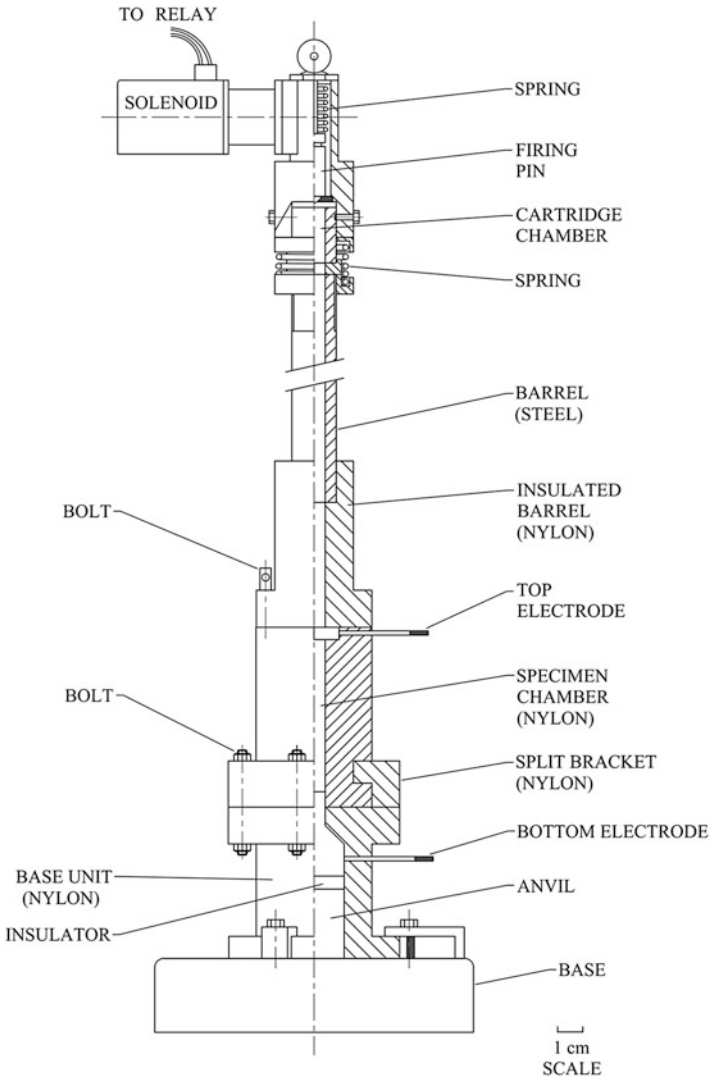

Fig. 3.27 Schematic of an electro impact compaction (EIC) apparatus. (Reprinted from Alp et al. [52], Copyright (1993) by permission of Taylor & Francis Ltd., www.tandfonline.com)

higher relative densities compared with consolidation by the electric discharge method only. An EIC apparatus shown in Fig. 3.27 consists of an assembly of a punch and a hammer, a pulse coil, and a steel casing. An insulating material separates the casing from the cylindrical high-voltage electrode. The low-voltage electrode possesses an insulating cylinder. The powder is placed into a nonconducting die. The apparatus is fixed on a steel plate. A high-voltage capacitor bank can be charged up to 20 kV and is used together with an impact device. The coil

of a mechanical relay receives energy from a DC current generator. The pulse coil makes the hammer held by a spring to move. The current is measured by a Rogowski coil. The capacitor discharge induces the electromotive force in the toroid proportional to the current. The current is recorded by a digital oscilloscope. The hammer velocity is measured with the help of two optical fiber cables. The displacement of the hammer during the discharge is measured by a capacitor sensor.

3.5 High-Energy High-Rate (HEHR) Consolidation Setup

High-energy high-rate (HEHR) consolidation was developed in the USA and belongs to a group of processes, in which the electric energy evolves in the powder leading to its heating. The power levels pertaining to this method are of the order of 1 MJ s^{-1} [11]. In this facility, a homopolar generator is used, which transforms the energy of rotation into the electrical energy as a result of Faraday's effect (Fig. 3.28). The energy stored by the generator can reach 10 MJ. The homopolar generator can create current pulses of 100–500 kA, which are used to sinter the powder materials.

During the discharge, the current passing through the powder reaches maximum and then rapidly decreases to zero. An electric current waveform typical to the HEHR method is shown in Fig. 3.29. The voltage applied to the powder is <100 V. The pressure from a hydraulic press is applied for several minutes to provide time for the heat to be dissipated from the electrodes to the copper plates. The external pressure can reach 0.5 GPa. In Ref. [16], during consolidation of an aluminum alloy powder, the maximum current reached 100 kA after 200 ms. At the onset of the pulse, a pressure of 104 MPa was applied to ensure sufficient electrical conductivity of the powder. As the current pulse decayed, the pressure was stepped up to 207 MPa and held constant for another 5 min.

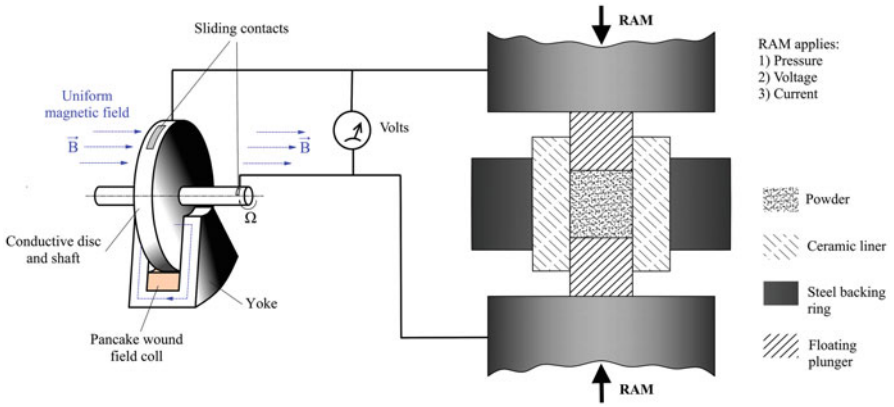

Fig. 3.28 Schematic of a HEHR setup. (Drawn using Refs. [11, 12])

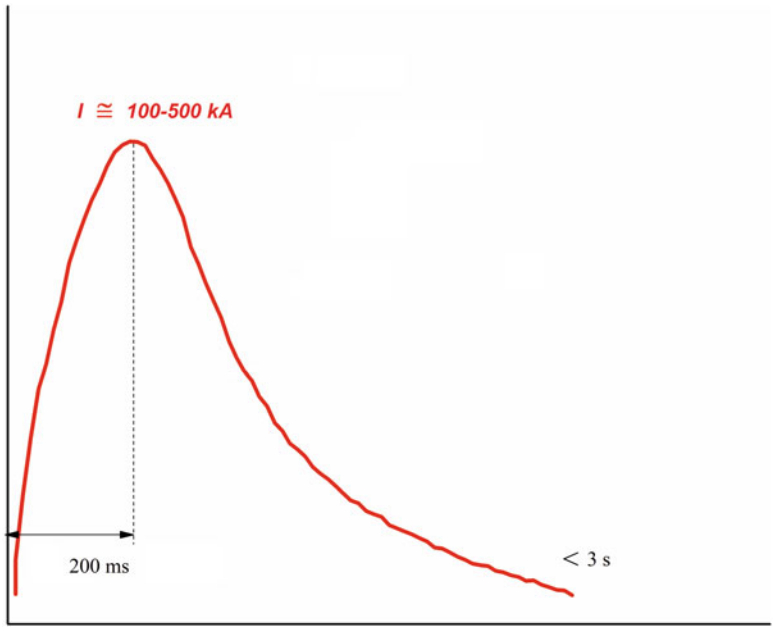

Fig. 3.29 Current waveform in HEHR. (Drawn using Ref. [11])

The die, electrodes, and contact surfaces of supporting rings are coated with boron nitride to prevent the formation of electric arcs during the process of consolidation. The die is a seamless tube made of corrosion-resistant steel. The electrodes are also made of steel. Another possibility is to work with an alumina die and protect it by a steel tube to prevent it from damage during sintering [14, 15].

3.6 Capacitor Discharge Sintering (CDS) Setup

Capacitor discharge sintering (CDS) was first used for consolidation of powders by Knoess and Schlemmer to produce dense compacts [19]. It was further studied and improved by Fais, who used it for making nearly fully dense metallic materials and metal–ceramic composites [21]. The CDS method uses two circuits coupled by mutual inductance instead of a single RLC circuit. This configuration allows applying low voltages to the powder compact thus reducing the possibilities of discharges, breakdown, and local plasma formation during the process. The CDS normally produces nearly fully dense compacts, the porosity being present only in the surface layer and uniformly distributed.

The CDS method is based on the storage of high-voltage electrical energy in a capacitor bank inserted in a freely oscillating system composed of a primary circuit and a mutually coupled secondary circuit (Fig. 3.30). The secondary circuit works in

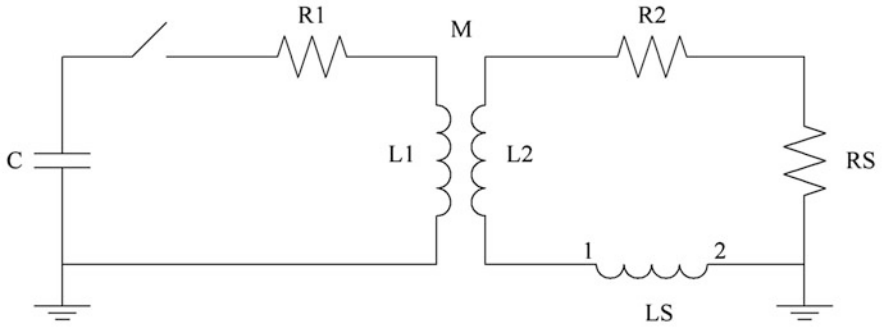

Fig. 3.30 Equivalent electric diagram of the CDS setup [21]

conjunction with a mechanical press, which is controlled by a programmed logical controller. Once the desired pressure from the press is reached, the switch closes the circuit, and the electromagnetic energy is transferred to the secondary circuit by means of a transformer that enables conversion from high voltage and low current in the primary circuit to low voltage and high current in the secondary circuit.

Knoess and Schlemmer [19] utilized a ceramic die as well as a conducting die with an insulating coating. The punches were made of molybdenum. The applied pressure was 1 GPa, while the voltage was less than 50 V. The powder was subjected to 1–2 pulses of current (100 kA) during 2–3 ms.

The main advantage of CDS is the reliability of the electric discharge system, which uses solid-state devices instead of ignitrons. The service life of the electronic components of the primary circle is more than 10^7cycles, which ensures reliable and reproducible discharges. When high energies are transferred to the powder compact, the applied voltage can be reduced by a transformer. In the primary circuit, the capacitors are charged up to voltages in the 1.5–3.5 kV range, whereas the current passing through the powder has a voltage of 5–50 V. A high voltage is transformed into a lower voltage during 2–3 ms, while the current pulse is 10–40 ms long. The current density can reach 100 MA mm^{-2}. The CDS does not normally use a protective atmosphere or vacuum. A schematic of a CDS setup and variation of the process parameters with time are presented in Fig. 3.31a.

In order to consolidate the powder, a certain amount of energy should be supplied to the material. In order for the powder to receive an optimal amount of energy during the discharge, the other elements of the circuit should possess an optimal electrical conductivity. This concerns the capacitors, transformers, cables, and electrodes. It has been proved that electrical conductivity can be improved by pre-pressing the powder compact before sintering. In order to decrease resistance, copper electrodes may be used. As pressure has to be applied during sintering, copper has to be replaced by an alloy. Fais uses electrodes made of the Cu–1% Co–0.5% Be alloy [21]. Schutte et al. [42] showed that the best results were obtained when the electrodes made of an oxide particle-strengthened alloy were used (ODSC3/11). Egan and Melody [53] suggested Cu–W protection for the electrodes.

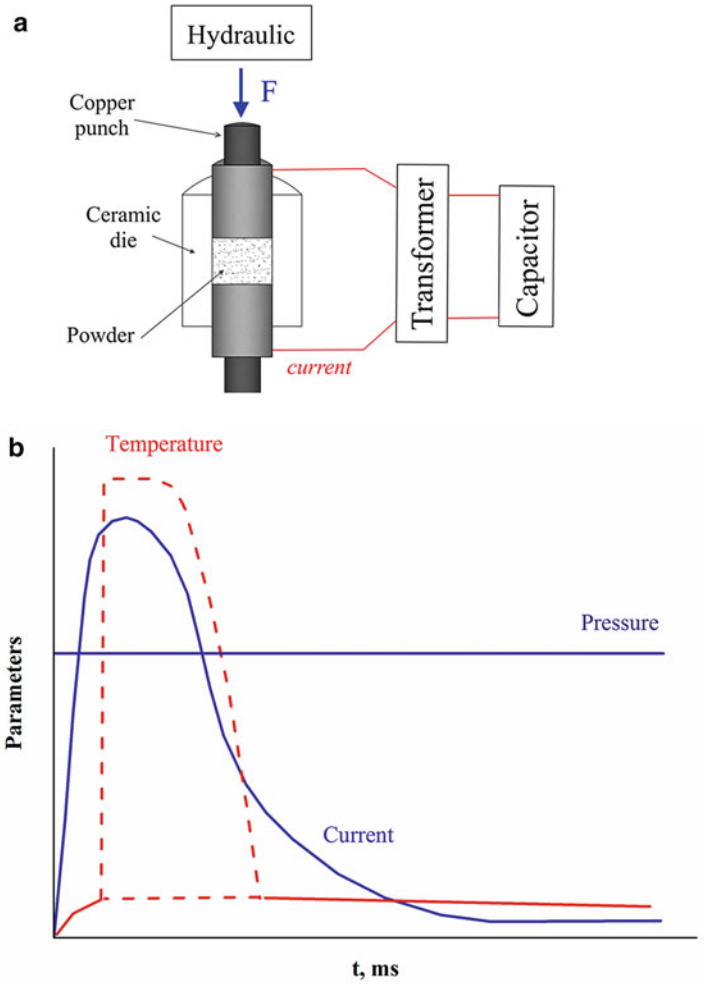

Fig. 3.31 Schematic of a CDS setup (**a**) and sintering parameters (**b**)

The temperature is measured by a pyrometer connected to a digital oscilloscope. The maximum temperature is reached in 10–30 ms, which indicates the end of the electric discharge (Fig. 3.31b). Cooling starts immediately after the discharge is finished and lasts for about 1 s. During sintering, the surface layers of particles melt at the microscopic level, while the integral temperature of the sample remains relatively low. The pressure applied to the sample is provided by a hydraulic press and reaches 1000 MPa. Schutte et al. used a hydraulic press with a possibility of increasing load stepwise (with a step of 1 kN) [42].

3.7 Pulse Plasma Sintering (PPS) Setup

Pulse plasma sintering (PPS) was developed at the Faculty of Materials Science and Engineering of Warsaw University of Technology, Poland [17, 18, 54–56]. The sintering technique used by Michalski and other researchers was initially called pulse electric discharge and was a predecessor of PPS. The consolidation process was carried out in two steps. The first step consisted of shaping the material at pressures up to 1 GPa at room temperature. At the second step, the pre-pressed sample 10 mm high and 10 mm in diameter was placed inside a setup, and a pressure of 1.2 GPa was applied [17]. Sintering was carried out in argon. The discharge of the capacitors (capacitance 200 μF) produces current pulses, which heat the sample. The pulse duration was 100 μs, while the pulse frequency was 0.5 Hz. The capacitors could be charged up to 7 kV. The punches (electrodes) carrying high current densities (of the order of $\approx 10\,\mathrm{MA/m^2}$) were made of titanium and aluminum. The current during the pulse reached several kA.

PPS uses pulses of electric current passing through the sample with a simultaneous application of pressure. The capacitor used in the setup has a capacitance of 300 μF with the maximum charging voltage of 10 kV. The powder is poured into a graphite die placed in between two graphite punches. The diameter of the die is 20 mm. The height of the samples can reach 15 mm. The pulse duration is usually several hundred of microseconds, while the current amplitude can reach several kA. The current source generates periodical pulses of current. The current pulse has an oscillating character similar to the other electric pulse sintering techniques. Arc discharges occur between the particles cleaning their surfaces and accelerating diffusion. The PPS process has high thermal efficiency. As the pulse duration (500 μs) is short in comparison to the interval between the pulses (1 s), the measured temperature is lower than that of the powder particle experiencing the action of the passing current, the latter possibly reaching several thousand degrees (Fig. 3.32). As a result, the process acquires a quasi-adiabatic character [54, 55]. Prior to sintering, the sample can be heated up to a selected temperature. PPS allows sintering of powders into compacts of relative densities exceeding 99%. Sintering is conducted in vacuum (Fig. 3.33), which differs this method from other methods based on the application of pulsed current. The samples are cooled in vacuum under applied pressure.

3.8 Briquetting by Electric Pulse Sintering

Pulsed current was suggested as a means to briquette dispersed metallic materials (Fig. 3.34) [57, 58]. In this case, pulsed current solves the problem of reclamation of metallic chips and other waste products of metallurgy. Materials for filters, getters,

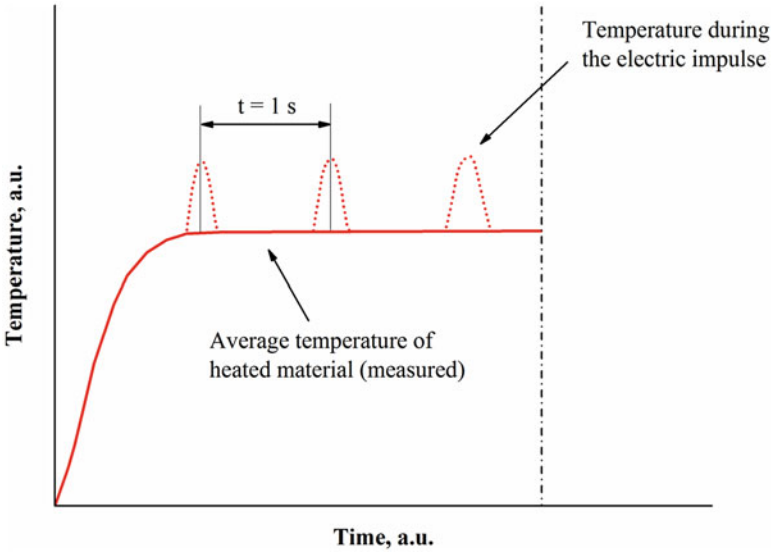

Fig. 3.32 Temperature variation during sintering by PPS. (Reprinted from Jaroszewicz and Michalski [54], Copyright (2005) with permission from Elsevier)

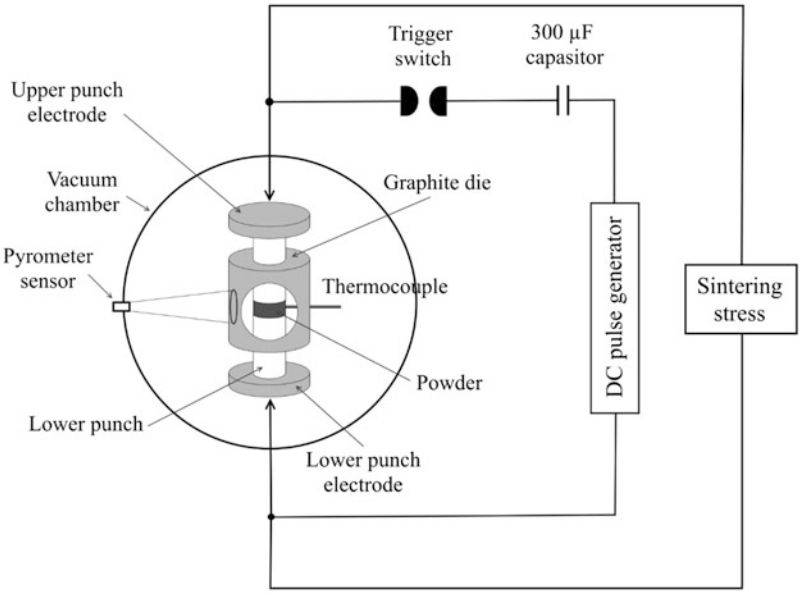

Fig. 3.33 Schematic of an apparatus for PPS. (Reprinted from Rosinski et al. [55], Copyright (2007) with permission from Elsevier)

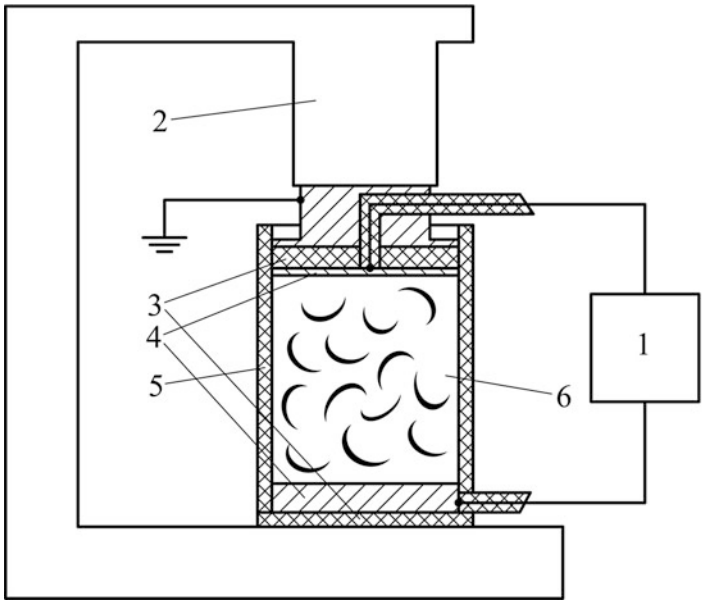

Fig. 3.34 A briquetting setup: 1, electric pulse generator; 2, press; 3, insulators; 4, punches (electrodes); 5, insulating die; 6, chips [58]

and acoustic and radio absorbers can be produced using the same technique. Composite briquettes containing inclusions of a different material can be manufactured; thus, briquettes with dielectric and electrically conducting inclusions can be made. The proposed pulsed current-based technology has been tried on chips of metals and alloys of varying quality; briquettes of various shapes have been obtained. The proposed technique includes pressing of the chips under a low pressure of 0.7–6 MPa in a nonconducting die. Keeping the pressure on the sample, electric current of high density is allowed to pass through it to form a briquette. The capacitor bank has a total capacity of 15 mF. The stored energy is 200 kJ, and the voltage is 5 kV. The current amplitude is 500 kA; the pulse duration is 250 μs. Briquettes with a diameter of 50 mm and heights ranging from 100 to 140 mm were obtained [57].

Metallic chips are pressed under relatively low pressures (up to 50 MPa, the remaining porosity is about 50%); then, keeping the pressure on the material, an electric pulse is allowed to pass through it resulting in the formation of a briquette. The material to be consolidated can be the waste consisting of metallic chips, powders, granules, or flakes including those coated with paint. Being pre-pressed only, the material remains weak and does not retain its shape after the pressure has been released. It is only with the application of electric current that the compact acquires strength and the ability to hold its shape.

3.9 Pulsed Current-Assisted Shock Consolidation

An interesting use of the capability of electric current to enhance consolidation has been found by Shvetsov et al. [59], who combined shock consolidation with a passage of a current pulse coming from a discharging capacitor connected to the consolidation ampoule. In Fig. 3.35, the setup for field-assisted shock compaction is shown for the consolidation with a central rod, which is common in shock wave technology. The powder was poured into a gap between the central rod and the inner wall of the ampoule. The ampoule was placed along the axis of a cylindrical charge of an explosive. Before the explosion, the central rod and the steel ampoule were connected to a high-voltage supply. The powder compact was insulated from the ampoule by a polyethylene film. After the capacitor was charged, the assembly was in the waiting mode. As the shock wave disrupted the insulation, an electric current passed between the ampoule and the central rod through the shock compressed powder.

The effect of the current pulse on the microstructure of the shock consolidated compact was significant: the part of the compact that was located closer to the capacitor was denser than parts located farther from the capacitor. The application of electric current has thus helped improve densification of what is known in the shock consolidation technology as a "cold" layer – a layer adjacent to the central rod and experiencing only moderate heating during shock consolidation. Evidence of melting of the central rod has also been found. The developed scheme offers a possibility to improve bonding between the central rod and the powder compact consolidated by shock waves.

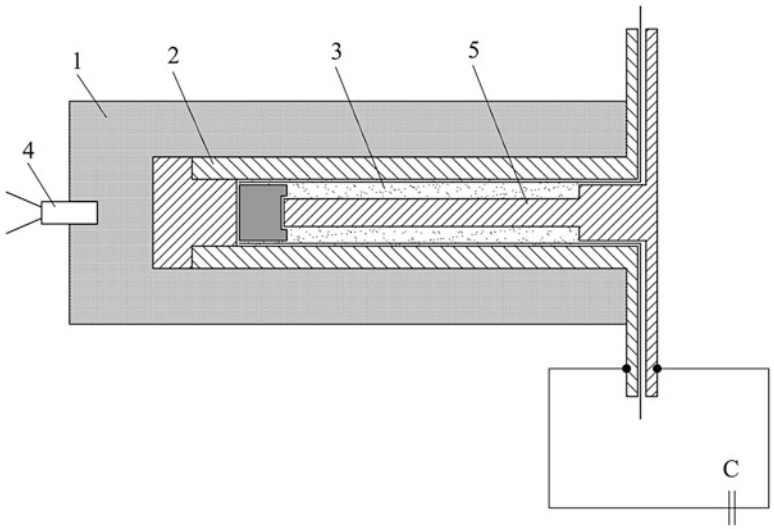

Fig. 3.35 Field-assisted shock consolidation setup: 1, explosive; 2, steel ampoule; 3, powder to be consolidated; 4, detonator; 5, central rod. (Drawn using data of Ref. [59])

3.10 Densification Kinetics Imposed by HVEDC

Since the governing parameters of the HVEDC technology are pressure and voltage, the densification map describing the density dependence on these two quantities can be built, as pictured in Fig. 3.36 for a ZrN powder [60]. The density of the specimens increases with the load applied in the pre-pressing stage. This trend appears, nevertheless, to have an upper bound. Given a value of electric current, a densification enhancement is observed up to a certain value of the cold-pressing load, after which any further increase affects density only slightly. Figure 3.36 also shows that the dependence of the relative density on the voltage is linear. The electric power is proportional to the squared voltage. If the voltage is applied for more than a few seconds, the zirconium nitride specimens can reach a thermodynamically stable structure. In this context, we expect the ZrN relative density to depend on the squared voltage. However, the extremely short duration of HVEDC processes leads to kinetically trapped structures, which renders the relative density linearly dependent on the applied voltage. A raise in the electric current density that flows through the powder compact leads to an increase in the density of the compact [60]. However, beyond a certain critical value, the powders will release a significant amount of voltage through the matrix. Quantitatively, the dependence between the energy and the voltage is complex, since the material resistance depends on the

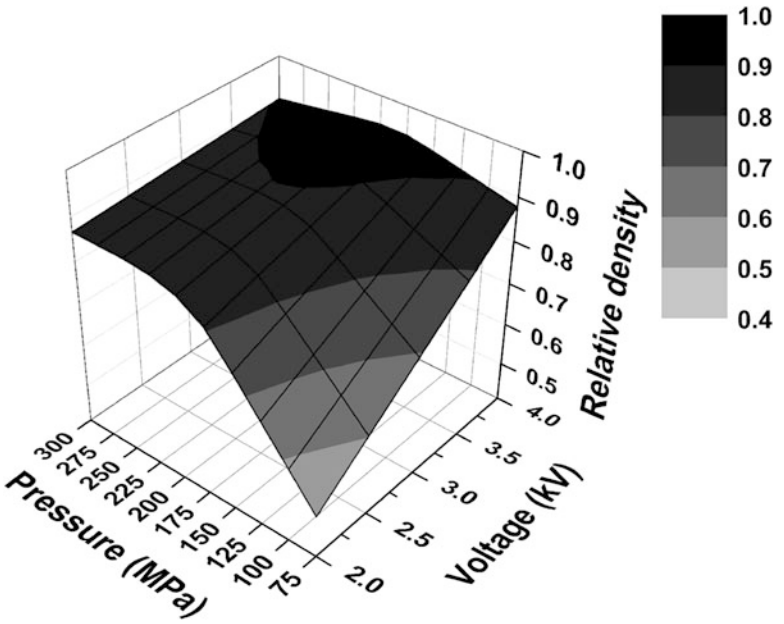

Fig. 3.36 The densification map of ZrN consolidated by high-voltage electric discharge consolidation. The relative density of the specimens is given as a function of pressure and voltage. The legend indicates the relative density. (Reprinted from Lee et al. [60], Copyright (2015) with permission from Elsevier)

relative density of the material, which evolves during the processing. In general, the dependences between the process energy and the instant values of system internal parameters, such as density, can be described by rather complex relationships, including exponential/logarithmic terms [60]. Therefore, it may be expected that, when explored over wider ranges of applied voltages, the relationship between the relative density and the voltage may become nonlinear.

It should be noted also that for the completeness of the conducted analysis, it is highly desirable to know the temperature of specimens according to the applied voltages. However, in its current apparatus' configuration, the temperature of specimens could not be measured during HVEDC process due to very short pulse duration.

The constitutive equation of the continuum theory of sintering [61] developed for hot pressing can be used to analyze the effect of electric currents on densification kinetics during HVEDC processes [60]. The constitutive equation for a nonlinear viscous material is [60, 61]:

$$\sigma_z = A_m \sqrt{\frac{2}{3}\frac{(1-\theta)}{\theta}(1-\theta)\left[\sqrt{\frac{2}{3}\frac{(1-\theta)}{\theta}}\left|\frac{\dot{\theta}}{(1-\theta)}\right|\right]^m} \tag{3.16}$$

where σ_z is the load applied (Pa), θ is porosity (dimensionless), $\dot{\theta}$ is the porosity change with time (1/s), and m is the strain rate sensitivity exponent. The material constant A_m (Pa · s^m), which is a function of microstructure (principally reflecting the influences of the grain size, sub-grain size, and dislocation density), is expressed by an Arrhenius-type relationship [60]:

$$A_m = A_{m0} T^m \exp\left(\frac{m\Delta H_{SD}}{RT}\right) \tag{3.17}$$

where A_{m0} is a material's constant (Pa·(s/K)^m), T the absolute temperature (K), ΔH_{SD} is the activation energy for self-diffusion (J/mol), and R is the gas constant (J/mol•K).

The sintering mechanism is related to the strain rate sensitivity m. For HVEDC, a significant aspect to be taken into account for the modeling of the process is the extreme rapidity characterizing this technique, which allows powders to be consolidated within a few seconds. A "zero-order approximation" of such technology based on its peculiarly short processing time can disregard the influence of heat on densification and, in view of the applied high pressures, can describe HVEDC as a cold-pressing process.

From the constitutive equation for the cold-pressing case, the following relationship can be derived [61]:

$$\sigma_z = \sigma_y \sqrt{\frac{2}{3}\frac{(1-\theta)^3}{\theta}} \tag{3.18}$$

where σ_y is the yield stress of the bulk material.

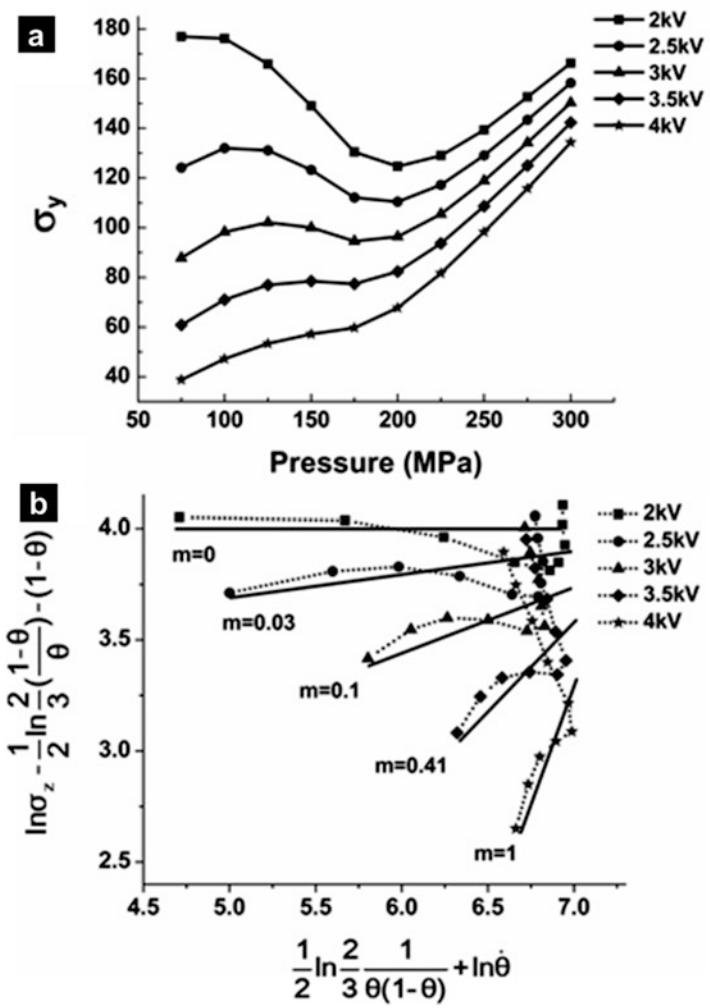

Fig. 3.37 Constitutive equation fitting of high-voltage electric discharge consolidation results. (**a**) yield stress variation with pressure and (**b**) m variation with voltage. (Reprinted from Lee et al. [60], Copyright (2015) with permission from Elsevier)

By substituting the experimental data on pressure and final porosity into Eq. (3.18), the yield stress for each condition can be calculated, as shown in Fig. 3.37a. It appears that when a low voltage is applied, Eq. (3.18) provides good correlations with experimental data for a constant value of the yield stress of the bulk material. Indeed, in low-voltage processes the short sintering time does not allow enough time for the effect of heating to be significant, and the adoption of a cold-pressing model can be considered adequate. When the voltage is increased, the high electrical currents are involved, and the consequent increased heat and/or

field-related phenomena compromise the validity of the purely plastic material assumption, inducing a pressure-dependent behavior on the "apparent yield stress."

The constitutive equation for a nonlinear viscous material, Eq. (3.16), was applied to the HVEDC results to determine the densification mechanism (m value). Taking the natural logarithm of Eq. (3.16) and rearranging,

$$\ln \sigma_z - \frac{1}{2} \ln \frac{2}{3} \left(\frac{1-\theta}{\theta} \right) - (1-\theta) = m \left\{ \frac{1}{2} \ln \frac{2 \quad 1}{3\theta(1-\theta)} + \ln \dot{\theta} \right\} + \ln A_m \quad (3.19)$$

After inserting the average porosity rate by calculating slope and pressure given in Fig. 3.36 into Eq. (3.19), a plot can be generated to determine m, as shown in Fig. 3.37b. In the conventional sintering theory, the densification of a powder by means of hot pressing provides 1 m value that is associated with a specific sintering mechanism. However, Fig. 3.37b shows mostly an increase of the slopes (m value) with increased voltage. Under low voltage, $m = 0$, which confirms that HVEDC acts like quasi-cold pressing. Increasing the voltage leads to a change of the strain rate sensitivity value m from 0 to 1, which is attributed to the increasing heat generation.

It appears that the combination of high pressure and voltage during HVEDC induces a different behavior in the material with respect to those used for modeling of hot pressing. The obtained first-order approximation provides an impetus for future work on refining the mechanisms underlying the novel and still rare technology of HVEDC.

3.11 Selected Examples of Materials Processed by High-Voltage Electric Pulse Consolidation

WC–Co composites were successfully sintered by HVEDC, as reported in Refs. [6, 7, 9]. Figure 3.38 shows the dependence of the relative density of the sintered material on the peak current density. The WC–Co composite has the maximum density when the peak current density reaches 95 kA cm^{-2}. When the current density exceeds 100 kA cm^{-2}, the density of the compact dramatically decreases.

Fais [21] showed that 99% dense WC–Co composites can be produced by CDS starting from a powder mixture containing 88% WC with a particle size of 120 nm and 12% Co and using a discharge power of 30 kJ. Siemiazko et al. [62] used PPS to conduct self-propagating high-temperature synthesis in the W–C–Co mixtures. The synthesized material showed a 30% increase in hardness relative to the material sintered from the mixtures of tungsten carbide and cobalt. Sintering was performed at 1500 K. Figure 3.39 shows the evolution of hardness, relative density, and grain size of the WC–Co composites with the sintering time; Fig. 3.40 demonstrates the variation of fracture toughness of the composites sintered for different times. The highest fracture toughness was achieved in the samples sintered for 10 min. With increasing sintering time, the fracture toughness degraded.

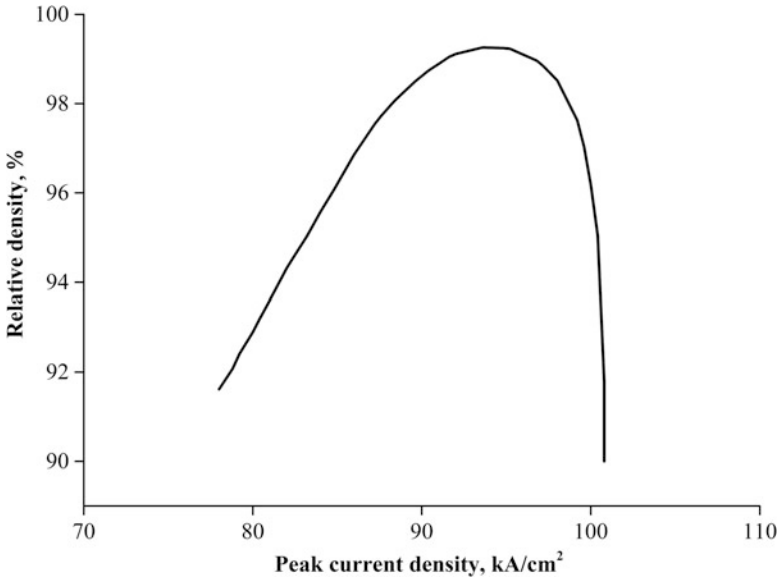

Fig. 3.38 Relative density of the sample vs. current density for WC-Co composites processed by HVEDC (applied pressure 200 MPa). (Reprinted from Grigoriev and Rosliakov [7], Copyright (2007) with permission from Elsevier)

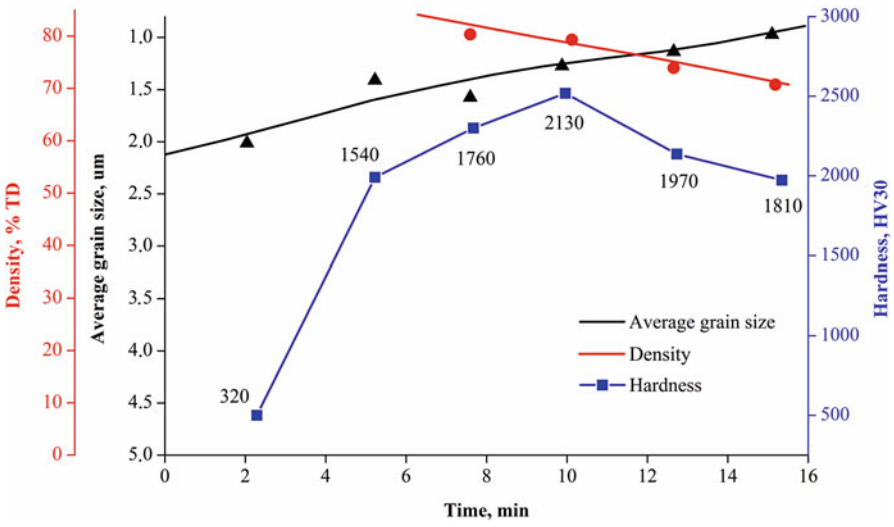

Fig. 3.39 Hardness, relative density, and grain size of WC–Co composites obtained by PPS vs. sintering time. (Drawn using data of Ref. [62])

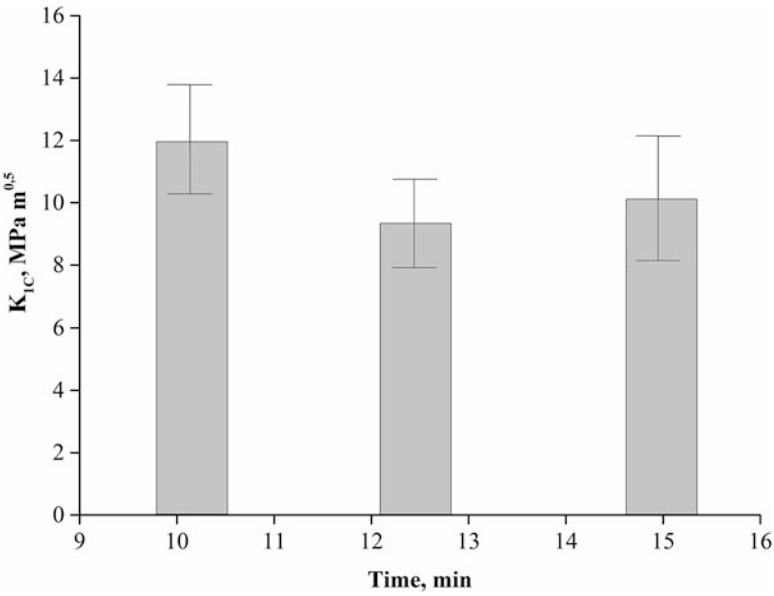

Fig. 3.40 Fracture toughness K_{IC} of WC–Co composites sintered by PPS for different times. (Drawn using data of Ref. [62])

Pulsed electric current can assist in the preparation of complex composite materials, which are challenging to produce by other methods. Thus, cBN/WC–Co composites with high strength and hardness were successfully produced by PPS [63]. The composites were obtained by sintering of WC + 0.5 wt.%VC + Co + cBN in vacuum at a temperature of 1100°C under an applied pressure of 100 MPa for 5 min.

The composites were not fully dense having densities of 92.6% and 98.6%, while the density of the material sintered without any addition of cubic BN was much higher (99.5%). The fracture surface of the sintered composites revealed transgranular fracture of the cBN particles (Fig. 3.41), which indicated strong bonding at the cBN/WC–Co interface.

Another example of sintering of a multiphase composite is consolidation of diamond/WC6Co by PPS [56] from a mixture of WC–6 wt.% Co (average particle size 0.8 μm) and diamond particles ranging from 40 from 60 μm comprising 30 wt.% of the composite. The hardness of the sintered material was 23 GPa.

PPS was successfully applied to join a W–Cu composite material to a tungsten substrate [64]. The composite–substrate interface was free of cracks and pores; no delamination effects have been observed (Fig. 3.42). Technologies based on pulsed electric current are promising for the production of Cu–W composite stacks [12]. A copper foil and a tungsten grid were used as the initial components. The stack was pressed at room temperature and in ambient air. Keeping the pressure

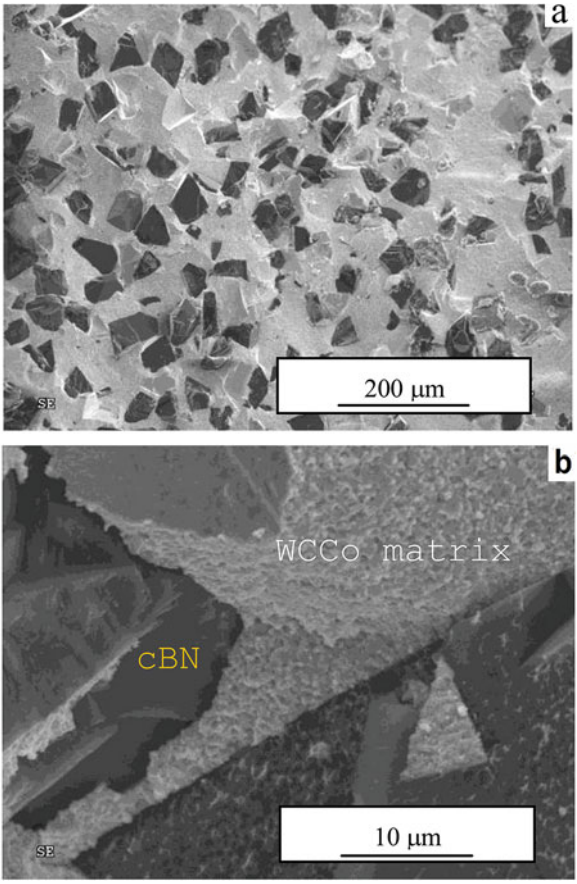

Fig. 3.41 Fracture surface of the 30 vol% cBN-(WC-0.5wt%VC-6wt %Co) composite ((**a**) microstructure, (**b**) interface between BN and the matrix). (Reprinted from Michalski et al. [63], distributed under Creative Commons Attribution (CC BY) license, https://creativecommons.org/licenses/by/3.0/)

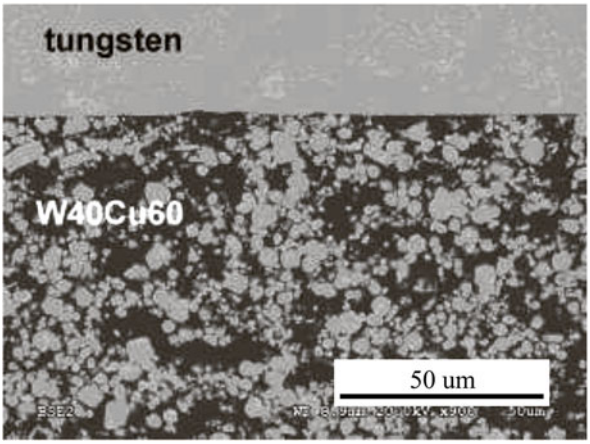

Fig. 3.42 W–Cu composite joined to a W substrate [64]

applied to the stack, a current pulse was allowed to pass through it. The resultant composite was 95% dense.

PPS was shown to be suitable for the sintering of Cu–diamond composites containing 50% of diamond [65]. Commercially available diamond powders were mixed with pure copper and a Cu–Cr alloy containing 0.8 wt.%Cr. High relative density and thermal conductivity of the Cu0.8Cr–diamond composite can be explained by the formation of chromium carbide at the metal–diamond interface. High thermal conductivity of the Cu0.8Cr–diamond composite makes it attractive for heat sink management in high-power circuits. Although sintering was carried out at a temperature, at which diamond is thermodynamically unstable, graphite was not found in the sintered samples.

The preparation of dense copper by CDS has been described in Ref. [23]. A copper powder with the particle size of 25 nm was used. Sintered by a discharge of 6 kJ, the compacts were 94–100% dense with a grain size of 26 nm and microhardness of 183 HVB.

Electric pulse sintering by a single discharge was used by Anisimov and Mali [35] to consolidate copper powders at current densities $\geq 10^2$ A mm^{-2} and pulse durations $\leq 10^{-4}$ s. Sintering was successful when the current integral (Eq. 3.7) exceeded its critical value $J^* = 1.4 \times 10^{15}$ A^{2}s m^{-4}, which is significantly lower than that required to cause complete melting of copper ($J^* = 1.05 \times 10^{17}$ A^{2}s m^{-4}). Nearly fully dense Cu monoliths were obtained. The same method was used to sinter Cu–40 vol.% TiB_2 composites and mixtures of Ti–B–Cu containing Ti and B in the amounts to form 40 vol.% TiB_2–Cu composites. Porous composites were obtained as a result of electric pulse sintering containing particles of TiB_2 20–40 nm in size distributed in the copper matrix. The critical value of the current integral was lower in the case of reactive sintering (Ti–B–Cu) due to an exothermic reaction between the components of the mixture ($Ti+2B=TiB_2$). Although the sintered composites maintained some porosity, their electric erosion resistance was four times greater compared with monolithic copper. These experiments have proved that electric pulse sintering is suitable for both reacting and non-reacting powder systems.

High-voltage electric discharges have been used to synthesize nanocrystalline intermetallics Nb_2Al and Nb_3Al from a mechanically alloyed mixture of Nb (77 wt.%) and Al (23%) [41]. The grain size of the mechanically alloyed material was 5–8 nm. The pre-pressed samples of 75–85% relative density (the external pressure was 450 MPa) were subjected to an electric discharge with a specific energy of 1 kJ g^{-1}. The two-phase material was 98% dense having grains from 26 to 36 nm and hardness ranging from 14.7 to 17.6 GPa.

An et al. [49] employed EEDS to produce implant materials. Sintered parts having a dense core and porous peripheral regions were obtained in a single step. They are suitable for the successful intergrowth with the bone tissue. The implants were sintered from an atomized titanium powder having particles 150–200 μm in size. An electric energy of 1.5 kJ was evolved in the 0.7 g of the Ti powder. The consolidation was performed in vacuum of about $\sim 2 \cdot 10^{-2}$ Torr. Figure 3.43 shows the surface and the cross-section of the sintered sample [49].

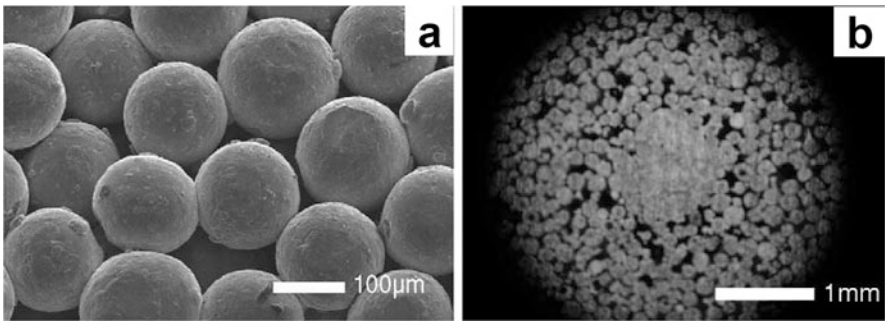

Fig. 3.43 Porous surface (**a**) and cross section (**b**) of the sintered Ti sample. (Reprinted from An et al. [49], Copyright (2005) with permission from Elsevier)

A review of the structure and properties of porous metallic materials produced using high-voltage consolidation was presented by Minko and Belyavin [66]. The electrical resistivity of consolidated metals was suggested as a convenient parameter to control the quality of inter-particle bonding after consolidation. The dependences of the electrical resistivity of the samples on the pressing pressure for titanium, niobium, and tantalum were similar. As the pressure increased, a drop in the resistivity of the samples was observed due to destruction of oxide films and the formation of good metallic contacts between the particles of the powder. After reaching a minimum, the resistivity started to increase with a further increase in the pressing pressure. This effect was explained by insufficient heating of the samples (at pressures greater than 20 MPa) during the consolidation (see Sect. 3.3).

3.12 Summary

High-voltage electric pulse sintering techniques have many characteristics common to other consolidation methods that use electromagnetic fields; however, several features pertaining to electric pulse sintering make it a self-standing area of powder metallurgy. High-voltage electric pulse sintering has potential to provide technological and economical benefits, which is possible due to the following process characteristics:

- Short process duration
- Fewer processing steps in comparison with other sintering methods (a possibility of combining shaping and sintering steps)
- Often palliated requirements for the sintering conditions (protective atmosphere or vacuum may not be necessary)
- A possibility of making parts of the desired shape

One of the main challenges of high-voltage electric pulse sintering is achieving a uniform microstructure of the material, which is a prerequisite for the uniformity of

the properties at a macro-level. In each particular case, however, optimal parameters of consolidation should be found, which is an exigent task. The relative density of the sintered material can vary in a wide range depending on the consolidation parameters.

High-voltage electric pulse sintering is a unique technology suitable for sintering of materials with a wide range of possible applications (from space industry to medicine), including:

- Materials based on iron, copper, nickel, refractory metals, metals of high reactivity that are easily oxidized, complex mechanically alloyed materials.
- Electric pulse sintering is promising for consolidation of Al- and Ti-based rapidly solidified alloys, which have oxide films on the surface.
- Dissimilar materials joined together (metal–ceramic composites and steel, composites with non-conductive inclusions).
- Materials for specific applications (metallic glasses, superconducting composites, high-strength materials, materials for filters, getters, acoustic absorbers), etc.

However, the list of materials that can be processed by electric discharge consolidation is limited as the electric current should pass directly through the powder sample. Another drawback of the method is the necessity of high-voltage equipment.

Overall, high-voltage electric pulse sintering is promising to improve the properties of structural materials by forming nanostructures. This is possible due to short sintering durations implying that only slight changes in the microstructure of the material will occur during the process. However, very high sintering rates make it difficult to control the process parameters. Indeed, due to the transient nature of many associated phenomena, the *control of non-equilibrium* concept is especially important for high-voltage electric pulse sintering compared with many other field-assisted sintering techniques.

References

1. Belyavin KE, Mazyuk VV, Min'ko DV, Sheleg VK (1997) Theory and practice of electric pulse sintering of porous materials. Minsk, Remiko, p 180 (in Russian)
2. Yurlova MS, Demenyuk VD, Dudina D, Lebedeva LY, Grigoryev EG, Olevsky EA (2014) Review: electric pulse consolidation: an alternative to spark plasma sintering. J Mater Sci 49:952–985
3. Olevsky EA, Aleksandrova EV, Ilyina AM, Dudina DV, Novoselov AN, Pelve KY, Grigoryev EG (2013) Outside mainstream electronic databases: review of studies conducted in the USSR and post-soviet countries on electric current-assisted consolidation of powder materials. Materials 6:4375–4440
4. Grigor'ev EG (2008) Kinetics of the consolidation processes in dispersed materials under electric-pulse effect. Bull Rus Acad Sci: Phys 72(9):1210–1212
5. Grigoryev EG, Olevsky EA (2012) Thermal processes during high voltage electric discharge consolidation of powder materials. Scr Mater 66:662–665
6. Grigoryev EG (2011) High voltage electric discharge consolidation of tungsten carbide-cobalt powder. In: Cuppoletti J (ed) Nanocomposites with unique properties and applications in

medicine and industry. InTech, Rijeka, pp 345–360 ISBN: 978-953-307-351-4. Available from: http://www.intechopen.com/books/nanocomposites-withunique-properties-and-applications-in-medicine-and-industry/high-voltage-electric-discharge-consolidation-oftungsten-carbide-cobalt-powder
7. Grigoriev EG, Rosliakov AV (2007) Electro–discharge compaction of WC–Co and W–Ni–Fe–Co composite materials. J Mater Process Technol 191:182–184
8. Popov VP, Grigor'ev EG, Novikov SV, Baidenko AA, Goucharov SV (1996) Mathematical modeling of the densification process in the electrical discharge sintering of copper-tin powder. Powder Metall Metal Ceram 35:32–35
9. Grigoryev EG (2009) Kinetics of densification processes of powder materials under electro pulse sintering. Arab J Sci Eng 34(1):29–33
10. Belyavin KE, Min'ko DV, Kuznechik OO (2004) Modeling of the process of the electric-discharge sintering of metal powder. J Eng Phys Thermophys 77(3):628–637
11. Marcus HL, Weldon WF, Persad C, Eliezer Z, Bourell D (1990) Controlling fundamentals in high–energy high–rate pulsed power materials processing of powdered tungsten, titanium aluminides and copper–graphite composites. In: Final technical report, Center for Materials Science and Engineering, Texas University, Austin
12. Persad C, Peterson DR, Zowarka RC (1989) Composite solid armature consolidation by pulse power processing: a novel homopolar generator application in EML technology. IEEE Trans Magn 25(1):429–432
13. Orth JE, Wheat HG (1997) Corrosion behavior of high energy high rate consolidated graphite/copper metal matrix composites in chloride media. Appl Compos Mater 4:305–320
14. Wang MJ, Persad C, Eliezer Z, Weldon WF (1987) High-energy/high-rate consolidation of copper-graphite composite brushes for high-speed, high-current applications. In: Gully JH (ed) Proc 3rd international conference on current collectors, paper 20, Austin, TX, USA
15. Eliezer Z, Wang MJ, Persad C, Gully J (1988) A novel processing technique for metal–ceramic composites. Mater Sci Forum 34-36:505–509
16. Elkabir G, Rabenberg L, Persad C, Marcus HL (1986) Microstructural evaluation of a high-energy high-rate P/M processed aluminum alloy. Scr Metall 20:1411–1416
17. Oleszak D, Jaroszewicz J, Rosinski M, Michalski A (2002) Structure of NiAl–TiC composite fabricated by mechanical milling and pulse electric discharge sintering. Rudy Metal 47:432–434
18. Rosinski M, Kruszewski M, Michalski A, Fortuna-Zalesna E (2011) W/steel joint fabrication using the pulse plasma sintering (PPS) method. Fusion Eng Des 86:2573–2576
19. Knoess W, Schlemmer M (1996) US Patent No 5529746
20. Fais A, Maizza G (2008) Densification of AISI M2 high speed steel by means of capacitor discharge sintering (CDS). J Mater Process Technol 202:70–75
21. Fais A (2010) Processing characteristics and parameters in capacitor discharge sintering. J Mater Process Technol 210:2223–2230
22. Scardi P, D'Incau M, Leoni M, Fais A (2010) Dislocation configurations in nanocrystalline FeMo sintered components. Metall Mater Trans A 41:1196–1201
23. Fais A, Leoni M, Scardi P (2011) Fast sintering of nanocrystalline copper. Metall Mater Trans A 27:1517–1521
24. Raichenko AI (1987) Basics of electric current-assisted sintering. Metallurgiya, Moscow, 128 p (in Russian)
25. Wu X, Guo J (2007) Effect of liquid phase on densification in electric–discharge compaction. J Mater Sci 42:7787–7793
26. Al-Hassani STS, Can M, Watson EJ (1986) A second order approximation to nonlinear circuit equations as applied to high energy electrical discharge processes. J Comput Appl Math 15:175–189
27. Alitavoli M, Darvizeh A (2009) High rate electrical discharge compaction of powders under controlled oxidation. J Mater Process Technol 209:3542–3549

28. Kim DK, Pak HR, Okazaki K (1988) Electro discharge compaction of nickel powders. Mater Sci Eng A 104:191–200
29. Zavodov NN, Kozlov AV, Luzganov SN, Polishchuk VP, Shurupov AV (1999) Sintering of metal powders by a series of strong current pulses. High Temp 37(1):130–135
30. Grigoryev EG (2009) Modelling of the macroscopic processes in powder medium under the powerful electric-pulse effect. Bulletin of the MSPU 1:52–56 (in Russian)
31. Clyens S, Al-Hassani STS (1976) Compaction of powder metallurgy bars using high voltage electrical discharges. Int J Mech Sci 18(1):37–40
32. Al-Hassani STS (1979) Consolidation of powder metallurgy bars by direct electrical discharge and rotary swaging. Wire Ind 46:809–816
33. Alp T, Darvizeh AF, Al-Hassani STS (1988) Preforming of metal-polymer composites by electric discharge compaction of powders. Powder Metall 3:173–177
34. Ervin DR, Bourell DL, Persad C, Rabenberg L (1988) Structure and properties of high energy, high rate consolidated molybdenum alloy TZM. Mater Sci Eng A 102(1):25–30
35. Anisimov AG, Mali VI (2010) Possibility of electric–pulse sintering of powder nanostructural composites. Comb Expl Shock Waves 46(2):237–241
36. Kim YH, Cho YJ, Lee CM, Kim SJ, Lee NS, Kim KB, Jeon EC, Sok JH, Park JS, Kwon H, Lee KB, Lee WH (2007) Self–assembled microporous Ti–6Al–4V implant compacts induced by electro–discharge sintering. Scr Mater 56:449–451
37. Arzt E (1982) The influence of an increasing particle coordination on the densification of spherical powders. Acta Metall 30(10):1883–1890
38. Sprecher AF, Mannan SL, Conrad H (1983) On the temperature rise associated with the electroplastic effect in titanium. Scr Metall 17(6):769–772
39. Vityaz' PA, Kaptsevich VM, Belyavin KE, Prezhina TE, Kerzhentseva LF, Govorov VG (1990) Contact formation during the electric-pulse sintering of a titanium alloy powder. Soviet Powder Metall Metal Ceram 29(7):527–529
40. Cho JY, Song GA, Choi HS, Kim YH, Kim TS, Lee MH, Lee HS, Kim HJ, Lee JK, Fleury E, Seo Y, Kim KB (2012) Necking mechanisms on porous metallic glass and W compacts using electro-discharge sintering. J Alloys Compd 536:S78–S82
41. Rock C, Qiu J, Okazaki K (1998) Electro-discharge consolidation of nanocrystalline Nb–Al powders produced by mechanical alloying. J Mater Sci 33:241–246
42. Schütte P, Moll H, Theisen W (2010) In: Proceedings of the PM2010 powder metallurgy world congress. European Powder Metallurgy Association, Florence
43. An YB, Oh NH, Chun YW, Kim YH, Kim DK, Park JS, Kwon JJ, Choi KO, Eom TG, Byun TH, Kim JY, Reucroft PJ, Kim KJ, Lee WH (2004) Mechanical properties of environmental electro discharge sintered porous Ti implants. Mater Lett 59:2178–2182
44. Grigoryev EG, Mitrofanov AV, Rosliakov AV (2000) In: Proceedings of the scientific session of MEPhI, part 9. Moscow, Russia (in Russian)
45. Belyavin KE (2000) Theoretical and technological bases of electric pulse sintering of refractory metal powders and application of the technology in industrial manufacturing of porous metallic parts. Synopsis of thesis, Research Institute of Powder Metallurgy with pilot production, Minsk (in Russian)
46. Bilalov BA, Kardashova GD, Magomedova EK, Ahmedov RR (2010) In: Proceedings of the international scientific and technical conference INTERMATIC–2010, part 2, Moscow, Russia (in Russian)
47. Bilalov BA, Gikitikchev MA, Magomedova EK, Dallaeva DS, Bilalov AB (2010) Process investigation of silicon carbide ceramic obtaining by electro pulse sintering. In the World of Scientific Discoveries (V mire nauchnyh otkrytiy) 6:191–193 (in Russian)
48. Jung J, Kim K, Lee W (2001) US Patent No 7347967
49. An YB, Oh NH, Chun YW, Kim DK, Park JS, Choi KO, Eom TG, Byun TH, Kim JY, Byun CS, Hyun CY, Reucroft PJ, Lee WH (2006) One–step process for the fabrication of Ti porous compact and its surface modification by environmental electro–discharge sintering of spherical Ti powders. Surf Coat Technol 200(14–15):4300–4304

50. An YB, Oh NH, Chun YW, Kim YH, Park JS, Choi KO, Eom TG, Byun TH, Kim JY, Hyun CY, Kim DK, Byun CS, Sok JH, Kwon JJ, Lee WH (2005) Surface characteristics of porous titanium implants fabricated by environmental electro–discharge sintering of spherical Ti powders in a vacuum atmosphere. Scr Mater 53:905–908
51. Lee WH, Hyun CY (2006) XPS study of porous dental implants fabricated by electro–discharge sintering of spherical Ti–6Al–4V powders in a vacuum atmosphere. Appl Surf Sci 252:4250–4256
52. Alp T, Can M, Al-Hassani STS (1993) The electroimpact compaction of powders: mechanism, structure and properties. Mater Manuf Process 8:285–289
53. Egan D, Melody S (2009) EDS as a method of manufacturing diamond tools. Met Powder Rep 64(6):10–13
54. Jaroszewicz J, Michalski A (2006) Preparation of a TiB_2 composite with a nickel matrix by pulse plasma sintering with combustion synthesis. Je Eur Ceram Soc 26:2427–2430
55. Rosinski M, Fortuna E, Michalski A, Pakiela Z, Kurzydlowski KJ (2007) W/Cu composites produced by pulse plasma sintering technique (PPS). Fusion Eng Des 82:2621–2626
56. Michalski A, Rosinski M (2008) Sintering diamond/cemented carbides by the pulse plasma sintering method. J Am Ceram Soc 91:3560–3565
57. Abramova KB, Bocharov YN, Samuilov SD, Shcherbakov IP (2001) Molding loose metal particles into briquettes with the use of short pulses of high density current. Tech Phys 46 (4):484–489
58. Samuilov SD (2002) Electrophysical method of briquetting of metallic scrap, Synopsis of thesis, Saint-Petersburg, Russia, 17 p. (in Russian)
59. Shvetsov GA, Mali VI, Bashkatov YL, Anisimov AG, Matrosov AD, Teslenko TS (2005) Effect of magnetic fields on explosive welding of metals and explosive compaction of powders. In: Schneider-Muntau HJ, Wada H (eds) Materials processing in magnetic fields, Proceedings of the international workshop on materials analysis and processing in magnetic fields, March 2004 in Tallahassee, Florida, World Scientific Publishing Co. Pte. Ltd., pp 360–370
60. Lee G, Yurlova MS, Giuntini D, Grigoryev EG, Khasanov OL, Izhvanov O, Back C, McKittrick J, Olevsky EA (2015) Densification of zirconium nitride by spark plasma sintering and high voltage electric discharge consolidation: a comparative analysis. Ceram Int 41:14973–14987
61. Olevsky E (1998) Theory of sintering: from discrete to continuum. Mater Sci Eng R 23:41–100
62. Siemiazko D, Michalki A, Rosinski M (2008) In: Skorokhod V (ed) Proceedings of symposium I "Functional and Structural Ceramic and Ceramic Matrix Composites (CCMC)", Warsaw, Poland
63. Michalski A, Rosiński M, Płocińska M, Szawłowski J (2011) Synthesis and characterization of cBN/WCCo composites obtained by the pulse plasma sintering (PPS) method. IOP Conf Ser Mater Sci Eng 18:202016 4 pages
64. Fortuna E, Rosiński M, Michalski A, Lisowski W (2007) FGM W-Cu composites and W-Cu/W joints fabrication route based on pulse plasma sintering (PPS) method. In: Annual report IPPLM, Warsaw University of Technology
65. Ciupiński L, Siemiaszko D, Rosiński M (2009) Heat sink materials processing by pulse plasma sintering. Adv Mater Res 59:120–124
66. Minko D, Belyavin K (2016) A porous materials production with an electric discharge sintering. Int J Refr Metals Hard Mater 59:67–77